The Recent Update of LS-DYNA Meshfree and Advanced FEM for Manufacturing Application

C. T. Wu, W. Hu*, Y. Guo

Livermore Software Technology Corporation

LS-DYNA© Forum, Bamberg Oct. 6th, 2014

Outline

- Part 1: Adaptive Meshfree Galerkin Method
  - Recent update on low-speed thermo-mechanical process
    - Motivations
    - Thermo-mechanical equations
    - Two-way adaptive procedure and remap algorithm
    - Implicit analysis using adaptive meshfree
  - Example: Friction Stir Welding (FSW) Simulation

- Part 2: Smoothed Particle Galerkin (SPG) Method
  - Application: severe deformation and failure analysis in solid
  - Numerical issues in conventional particle methods
  - Formulations and implementation
  - Benchmarks and numerical examples

Part 1

Adaptive Meshfree Galerkin Method
For Low-speed Thermo-mechanical Process

Motivation

- Numerical Challenges in low-speed thermo-mechanical process
  - Thermo-mechanical coupled problem
  - Large deformation ✓
  - Localized high-gradient field ✓ ✓
  - Free surface representation ✓
  - Frictional & thermal contact ✓
  - ? Material fusion ✓
  - ? Temperature-dependent material model
  - Residual stress analysis
  - Long processing time ✓ ✓

FEM

SPH

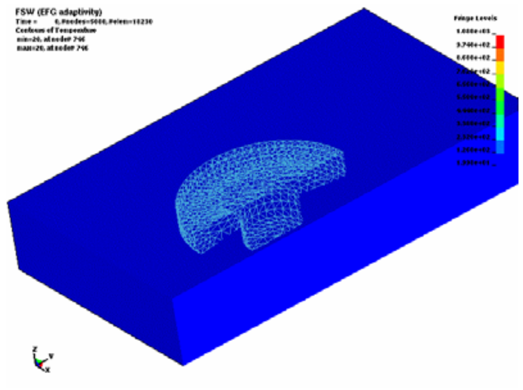

Motivation (Cont.)

- Adaptive Meshfree Galerkin Method
  - Large deformation

    EFG + Adaptivity
  - Localized high-gradient field

    High-order EFG approximation + Adaptive remapping function
  - Free surface representation

    Remesh + Local refinement
  - Frictional & thermal contact

    Mortar contact available In LS-Dyna
  - Material fusion ***Adaptivity***
  - Temperature-dependent material model ***Plasticity***
  - Long processing time

    Implicit solver

Thermo-mechanical equations

- Thermal Energy Conservation Equation

$$\rho C_p \dot{\theta} + \nabla \cdot \boldsymbol{q} = Q \quad in\ \Omega \times]0,T[$$

$$\boldsymbol{q} := -k(\nabla \theta) \qquad Q := \eta \boldsymbol{S} : \dot{\boldsymbol{\varepsilon}}^p$$

  - Boundary conditions

$$\theta = \theta_d \quad on\ \partial\Omega_d \times]0,T[$$

$$-\boldsymbol{q} \cdot \boldsymbol{n} = q_n \quad on\ \partial\Omega_n \times]0,T[$$

$$-\boldsymbol{q} \cdot \boldsymbol{n} = h_{cd}(\theta - \theta_{tool}) + \beta \boldsymbol{\lambda} \cdot \left[\dot{\boldsymbol{u}}^t \right] \quad on\ \partial\Omega_c \times]0,T[$$

$$-\boldsymbol{q} \cdot \boldsymbol{n} = h_{cv}(\theta - \theta_a) + h_r(\theta - \theta_a) \quad on\ \partial\Omega_{cr} \times]0,T[$$

  - Initial condition $\theta(\boldsymbol{X},0) = \theta_0(\boldsymbol{X}) \ in\ \Omega$

Thermo-mechanical equations (Cont.)

- Equation of Motion

$$\rho \ddot{\boldsymbol{u}} = \nabla \cdot \boldsymbol{\sigma} + \boldsymbol{b} \quad in\ \Omega \times]0,T[$$

- Boundary conditions

$$\boldsymbol{u} = \boldsymbol{u}_g \quad \text{on } \partial\Omega_g \times]0,T[$$

$$\boldsymbol{\sigma} \cdot \boldsymbol{n} = \boldsymbol{h} \quad on\ \partial\Omega_h \times]0,T[$$

- Contact conditions

$$\begin{cases} g \le 0 \\ -\boldsymbol{\lambda} \cdot \boldsymbol{n}^c = \lambda^n \ge 0 \\ \lambda^n g = 0 \end{cases} \qquad \begin{cases} \text{if } \|\boldsymbol{\lambda}^t\| < \mu(\theta)|\lambda^n| \text{ then } [\dot{\boldsymbol{u}}^t] = \boldsymbol{0} \\ \text{if } \|\boldsymbol{\lambda}^t\| = \mu(\theta)|\lambda^n| \text{ then } \exists \omega \ge 0 : [\dot{\boldsymbol{u}}^t] = \omega \boldsymbol{\lambda}^t \end{cases} \quad on\ \partial\Omega_c \times]0,T[$$

- Initial condition

$$\boldsymbol{u}(\boldsymbol{X},0) = \boldsymbol{u}_0(\boldsymbol{X}), \qquad \dot{\boldsymbol{u}}(\boldsymbol{X},0) = \dot{\boldsymbol{u}}_0(\boldsymbol{X})$$

Numerical Methods

- Lagrangian Formulation with Meshfree Discretization

$$u^h(X,t) = \sum_{I=1}^{NP} \Psi_I(X)\tilde{u}_I(t) \quad \forall X \in \Omega_X$$

$$\theta^h(X,t) = \sum_{I=1}^{NP} \Psi_I(X)\tilde{\theta}_I(t) \quad \forall X \in \Omega_X$$

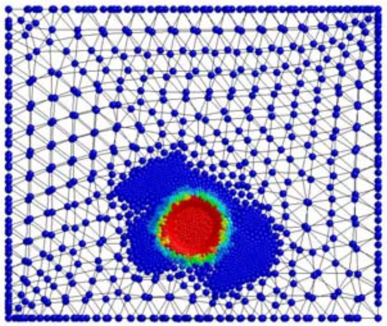

- *SECTION_SOLID_EFG
  - Normalized support size: 1.10

    Nodal density is considered to calculate the actual support
  - GMF approximation (IEBT=7): convex approximation
  - Gauss integration (IDIM=2) on background mesh
  - Pressure smoothing (IPS=1): enhance stress solution field

Numerical Methods (Cont.)

- Two-way Adaptive Procedure
  - Meshfree ***r*-**adaptivity

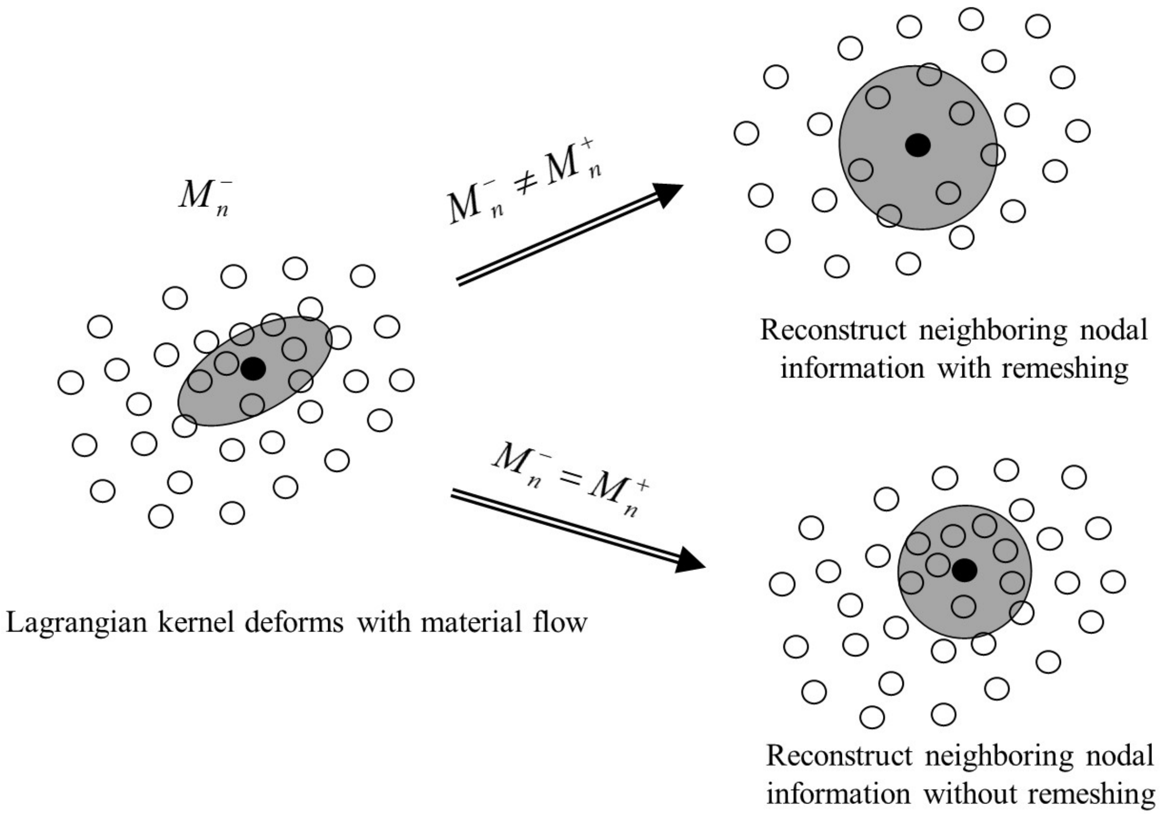

Numerical Methods (Cont.)

- Adaptive Solution Strategy

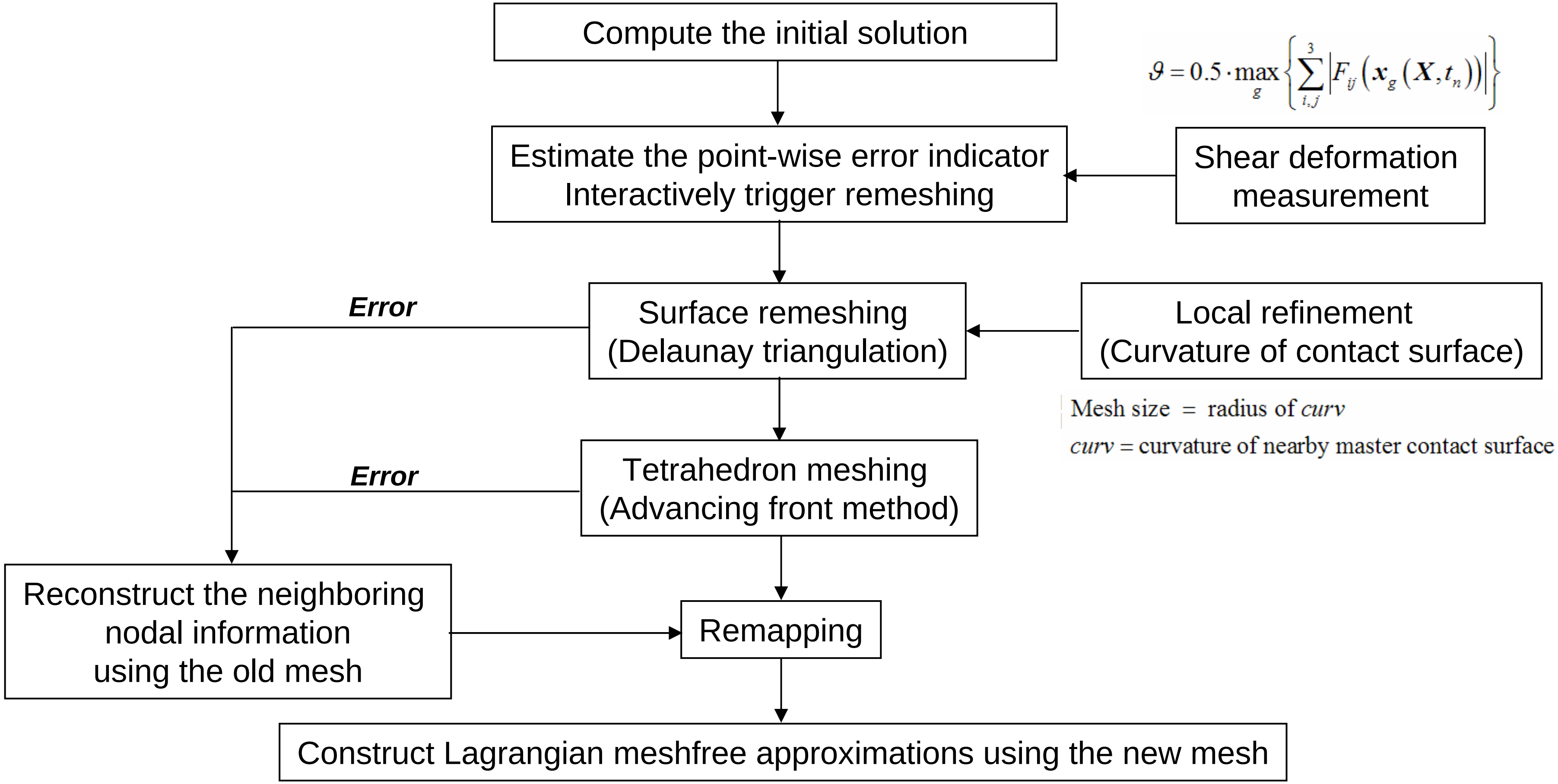

Numerical Methods (Cont.)

- Adaptive Remapping
  - Quantities at nodes

$$z_I^+\left(\boldsymbol{X}_I^+\right)=\sum_{J=1}^{NP^-}\Phi_J^-\left(\boldsymbol{X}_I^+\right)\tilde{z}_J^-\left(\boldsymbol{X}_J^-\right)\quad \forall \boldsymbol{X}_I^+\in M_n^+$$

$$\tilde{z}_J^-\left(\boldsymbol{X}_J^-\right)=\sum_{K=1}^{NP^-}\left(A_{JK}^-\right)^{-T} z_K^-\left(\boldsymbol{X}_K^-\right)$$

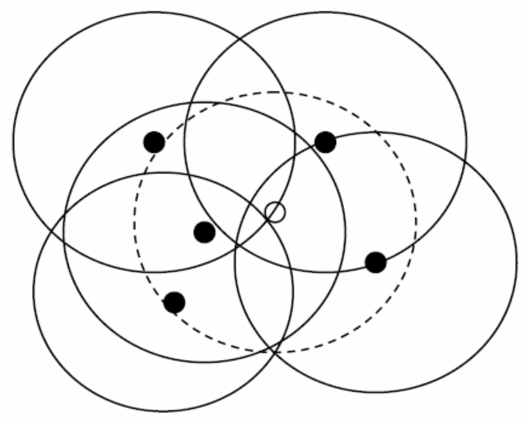

  - Internal variables at integration points

$$s_g^+\left(\boldsymbol{X}_g^+\right)=\sum_{j=1}^{mp^-}\varphi_j^-\left(\boldsymbol{X}_g^+\right)\tilde{s}_j^-\left(\boldsymbol{X}_j^-\right)$$

$$=\sum_{j=1}^{mp^-}\sum_{k=1}^{mp^-}\varphi_j^-\left(\boldsymbol{X}_g^+\right)\left(B_{jk}^-\right)^{-T} s_k^-\left(\boldsymbol{X}_k^-\right)$$

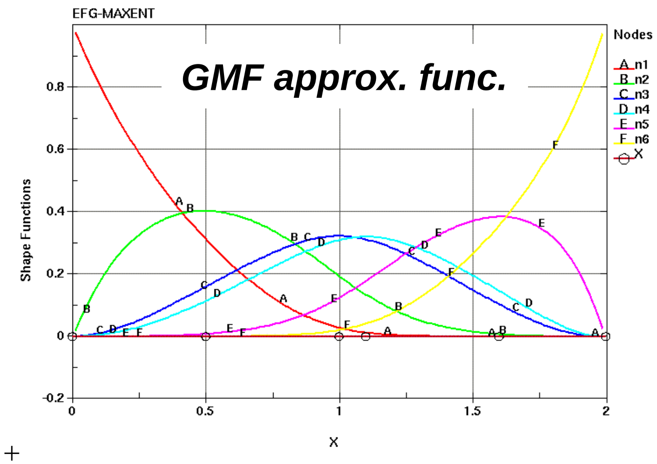

  - Second-order accurate in space

    Quantities remain unchanged if $M_n^- = M_n^+$

FSW Example

- Friction Stir Welding Process
  - Innovative consolidated welding technique:
    - Aluminum alloys, Cooper, Magnesium

      Low-melting point metallic materials
    - Repeatability

      Limited energy consumption

      Ease of automation
  - Four basic phases
    - Plunge
    - Stir
    - Weld
    - Retract

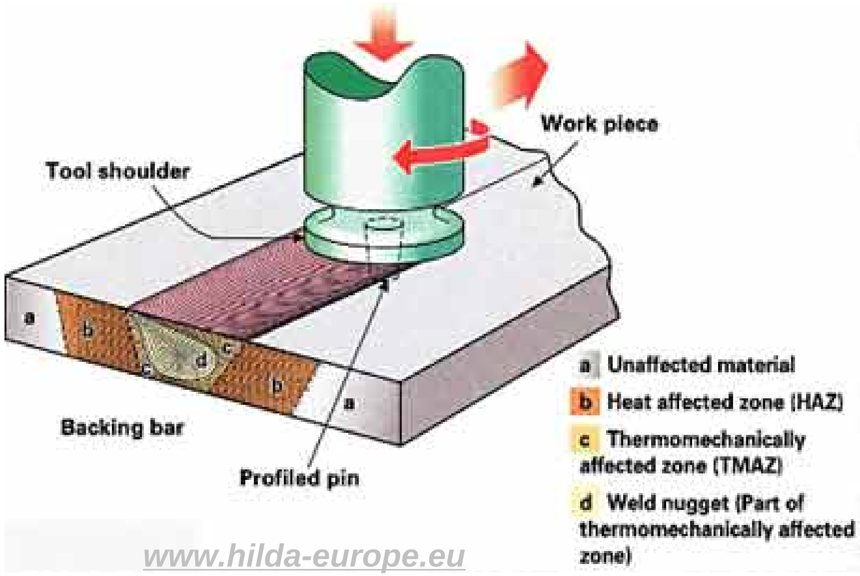

FSW Example (Cont.)

- Model

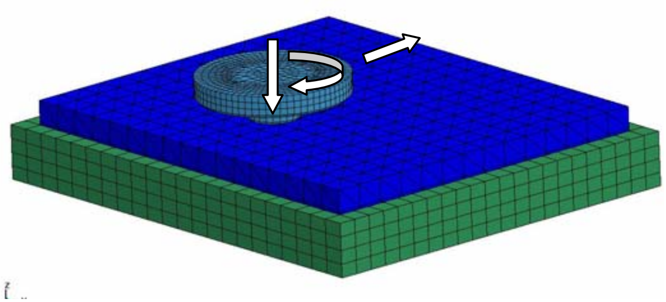

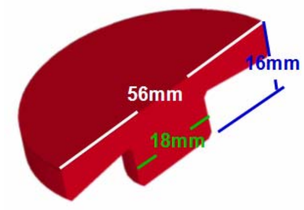

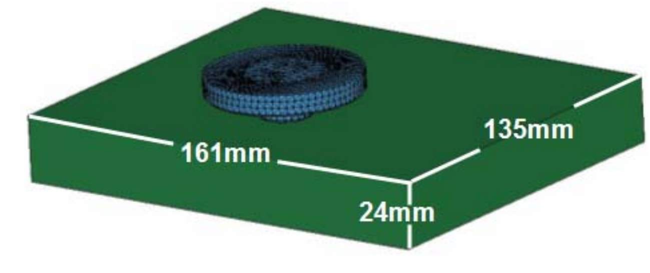

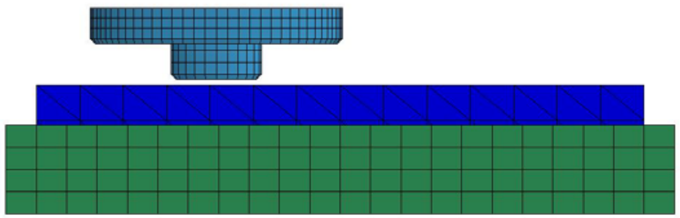

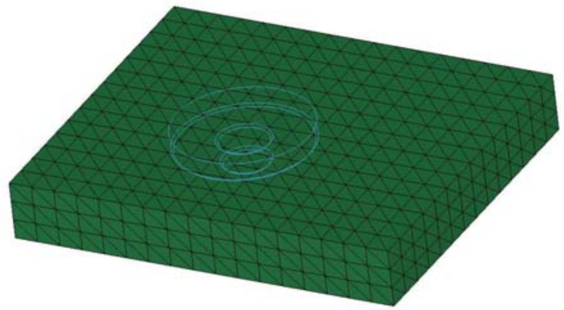

FSW Example (Cont.)

- Material
  - Work piece: Temperature dependant ideal plasticity

Table 1. Material parameters

	Density $(kg \cdot m^{-3})$	Thermal (Isotropic) Heat capacity $(J \cdot kg^{-1} \cdot {}^{o}C)$	Thermal (Isotropic) Thermal conductivity $(W \cdot m^{-1} \cdot K^{-1})$	Young's Modulus (GPa)	Poisson's ratio
Tool	7850	434	60	*rigid*	
Work piece	2700	875	175	70	0.3

Table 2. Yield stresses of the work piece

Temperature $({}^{o}C)$	20	100	300	550	800	1080
σ_y (MPa)	324	300	253	196	131	70

FSW Example (Cont.)

- Tool Motion
  - Rotating speed $125\ rad \cdot s^{-1}$

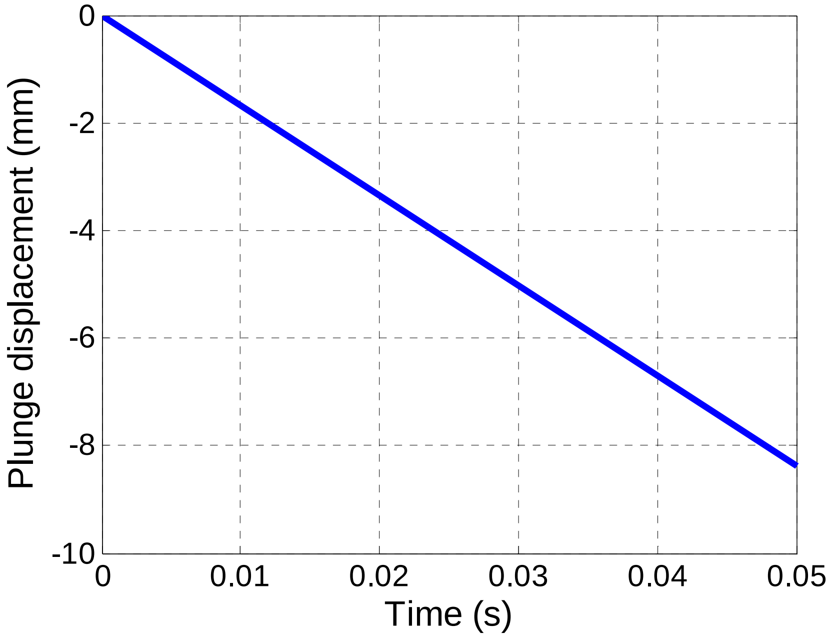

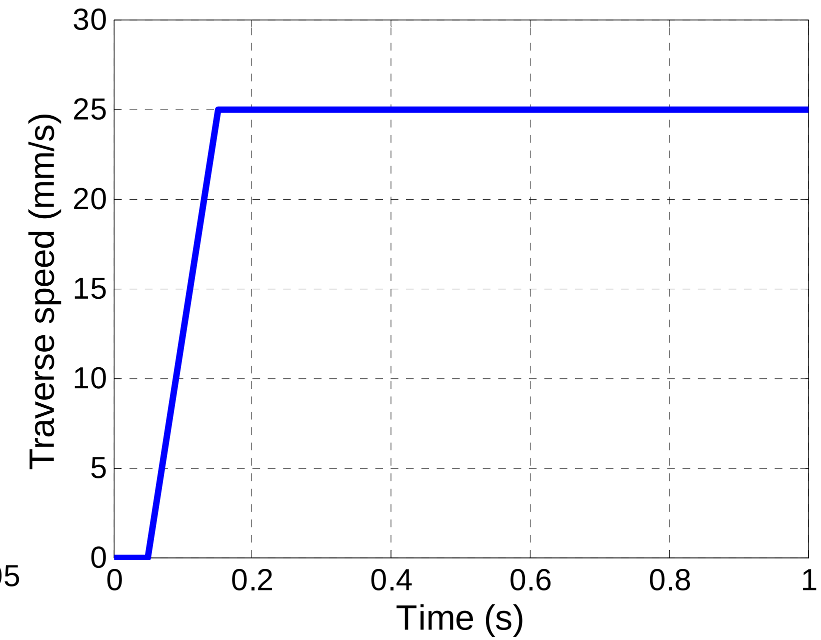

FSW Example (Cont.)

- Mortar Contact
  - FORMING_SURFACE_TO_SURFACE_MORTAR_THERMAL
    - Segment based penalty contact
    - Coulomb's frictional coefficient 0.7
  - Robust and efficient in implicit analysis
- Local Refinement
  - Master surface (tool) is modeled by shell: trigger local refinement
  - Tool is modeled by solid elements: compute temperature distribution
  - *CONSTRAIN_EXTRA_NODES_SET: constrain shell and solid parts
  - Integration cell size: 1*mm* and 8*mm*
- Implicit Analysis
  - IAUTO=1: maximum time step is 0.5*ms*
  - Termination time: 1s

FSW Example (Cont.)

- Computational time: 17 hours

  MPP double precision, 4 processors, Xeon E5520 2.27GHz
- Number of adaptive steps: 500
- Number of integration cells: Initially ~ 4000, increased to ~ 130000

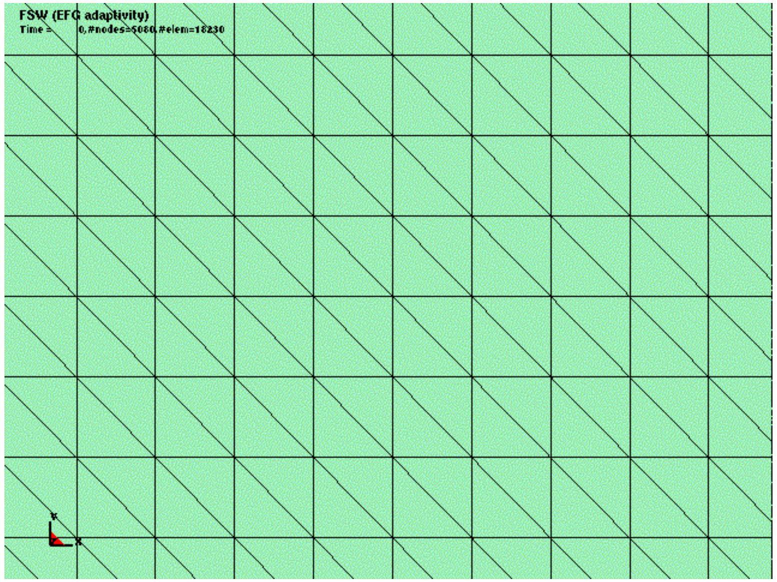

FSW Example (Cont.)

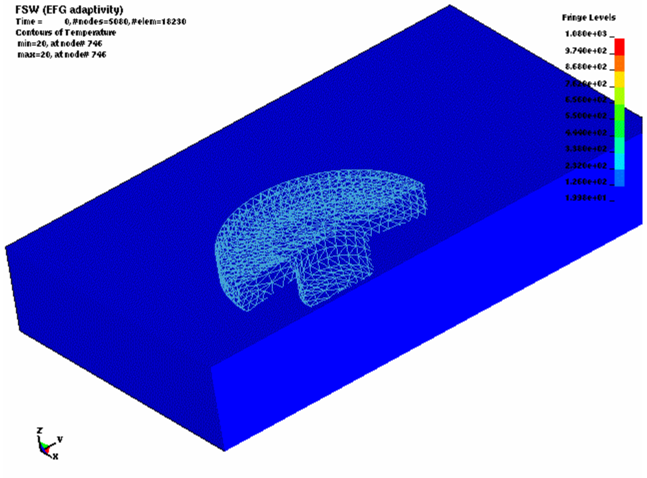

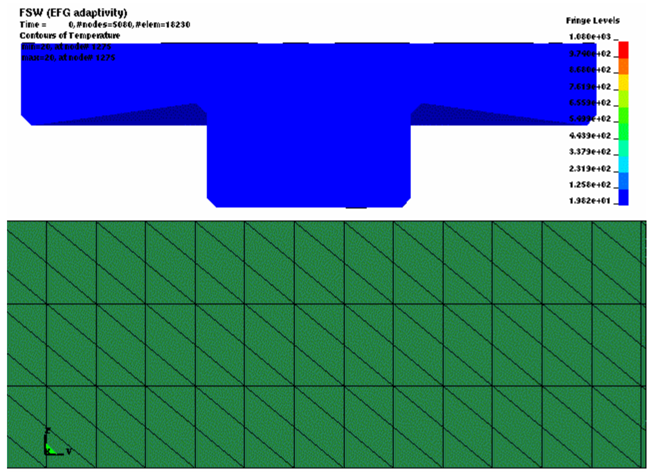

Temperature

Temperature

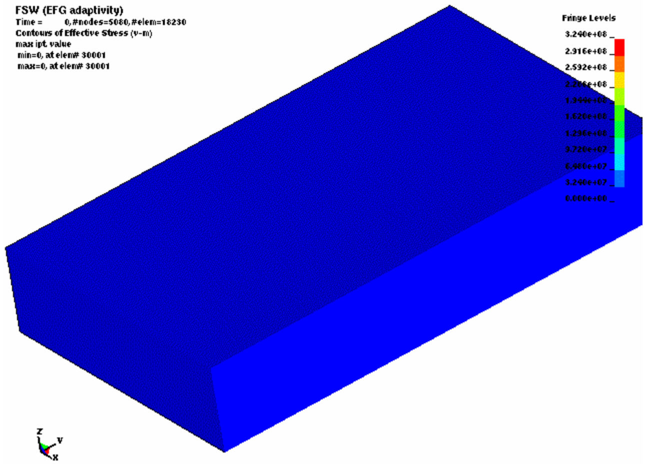

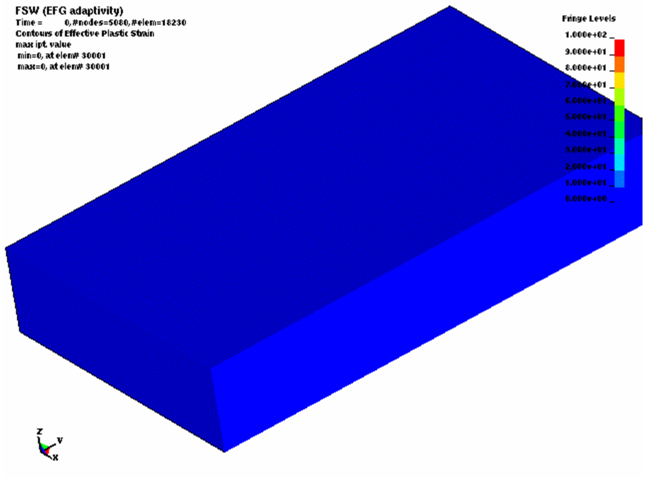

von mises stress

EPS

FSW Example (Cont.)

- Plunging Stage

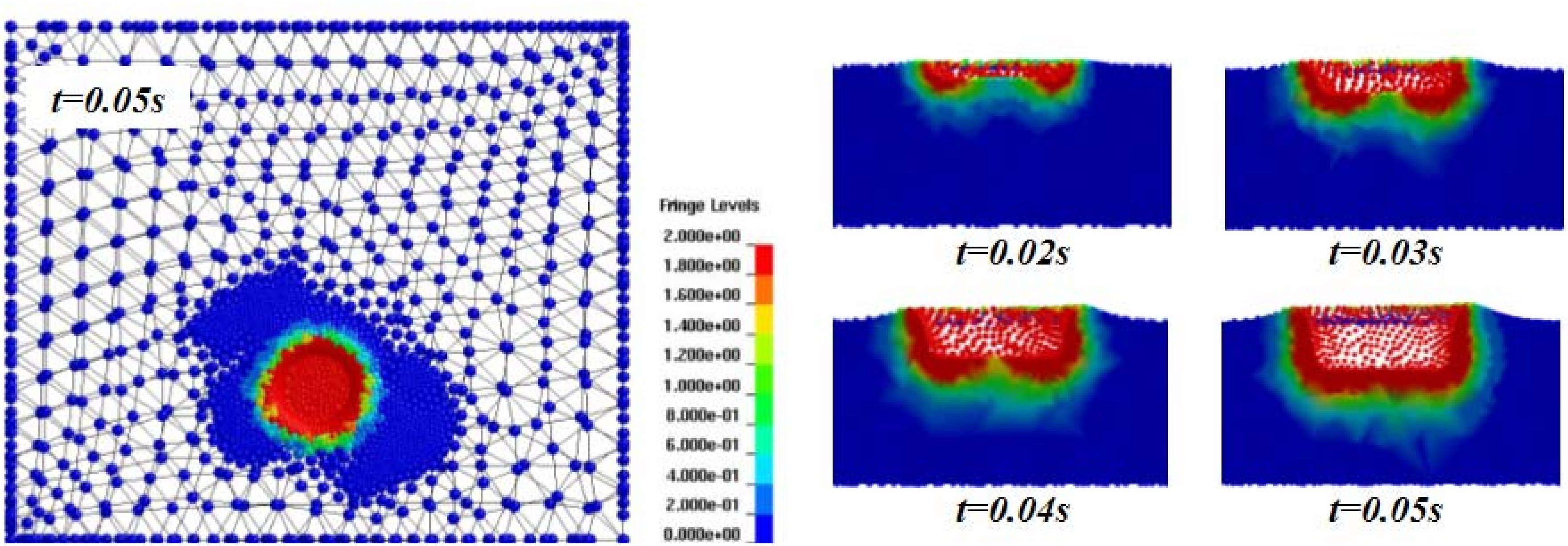

EPS

FSW Example (Cont.)

- Welding Stage

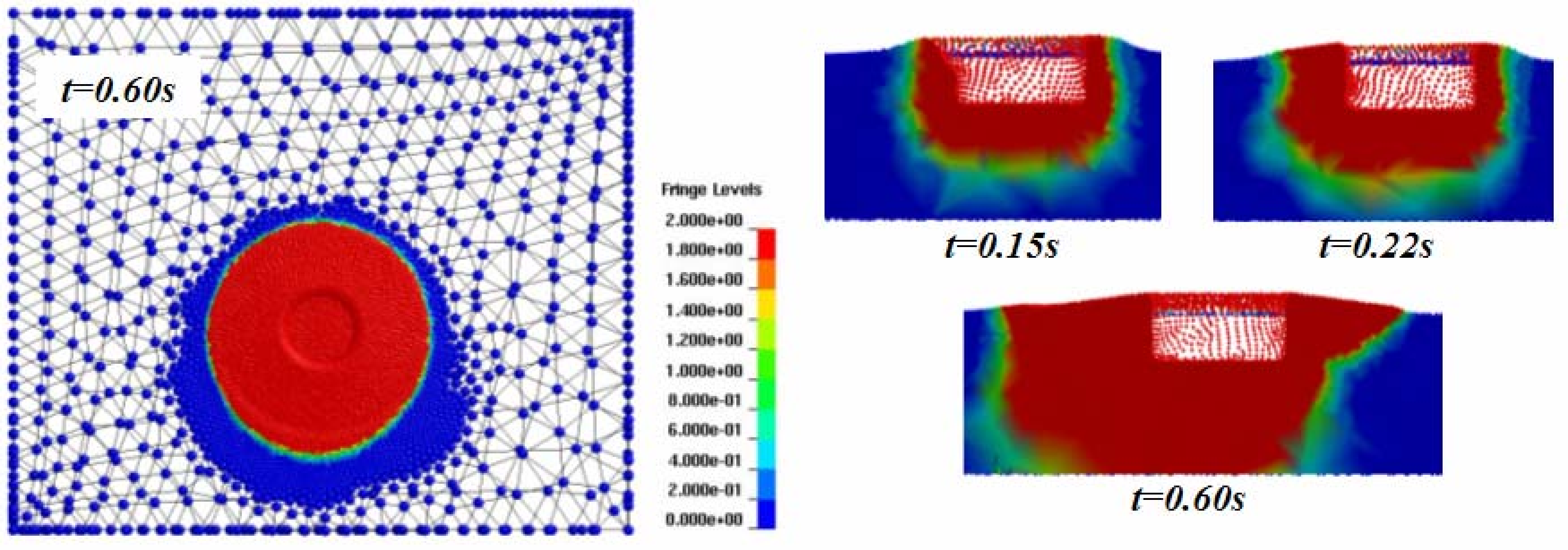

EPS

FSW Example (Cont.)

- Temperature

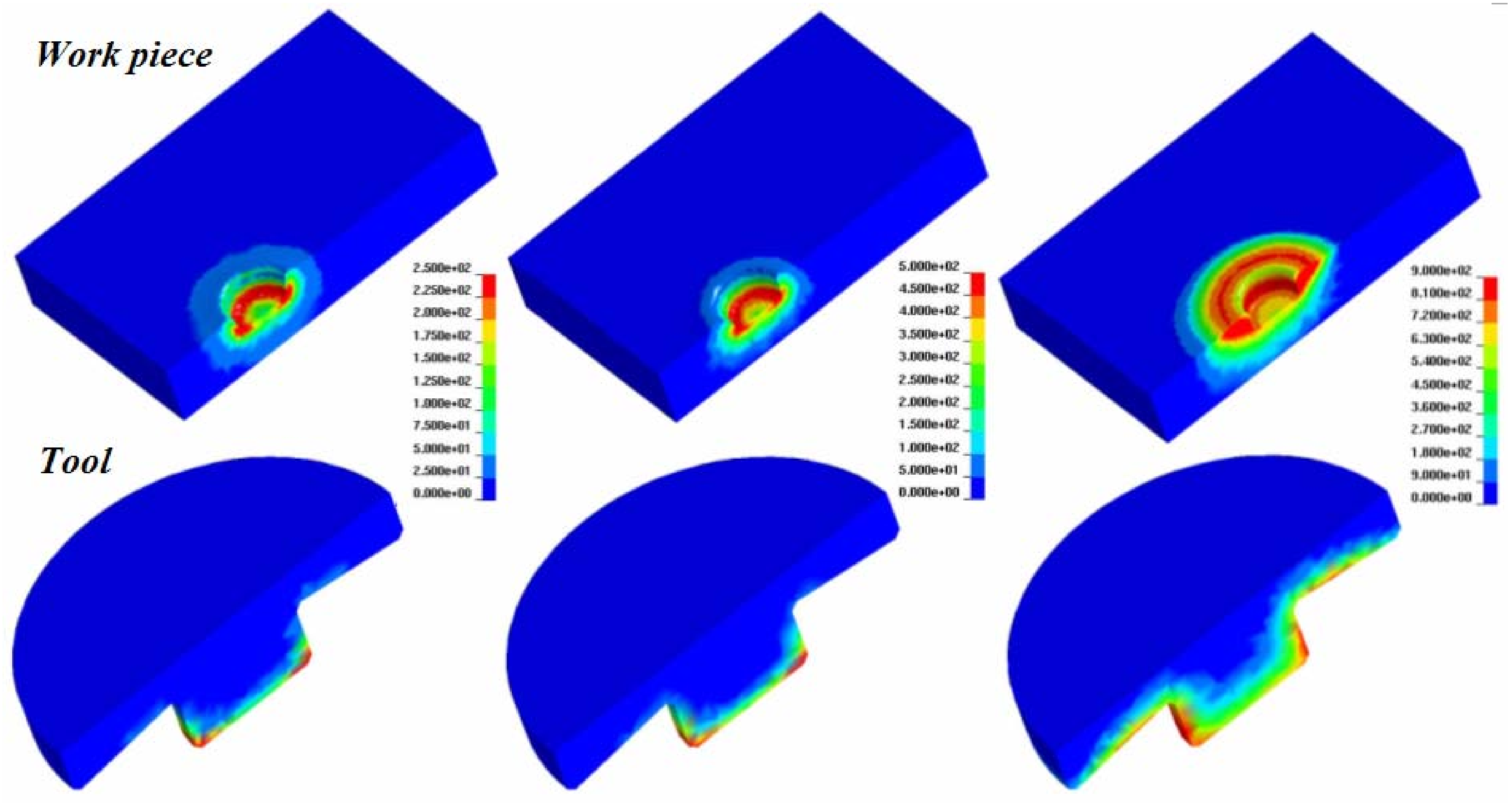

(a) *t=0.05s* (b) *t=0.15s* (c) *t=0.6s*

FSW Example (Cont.)

- Material Softening

von mises stress

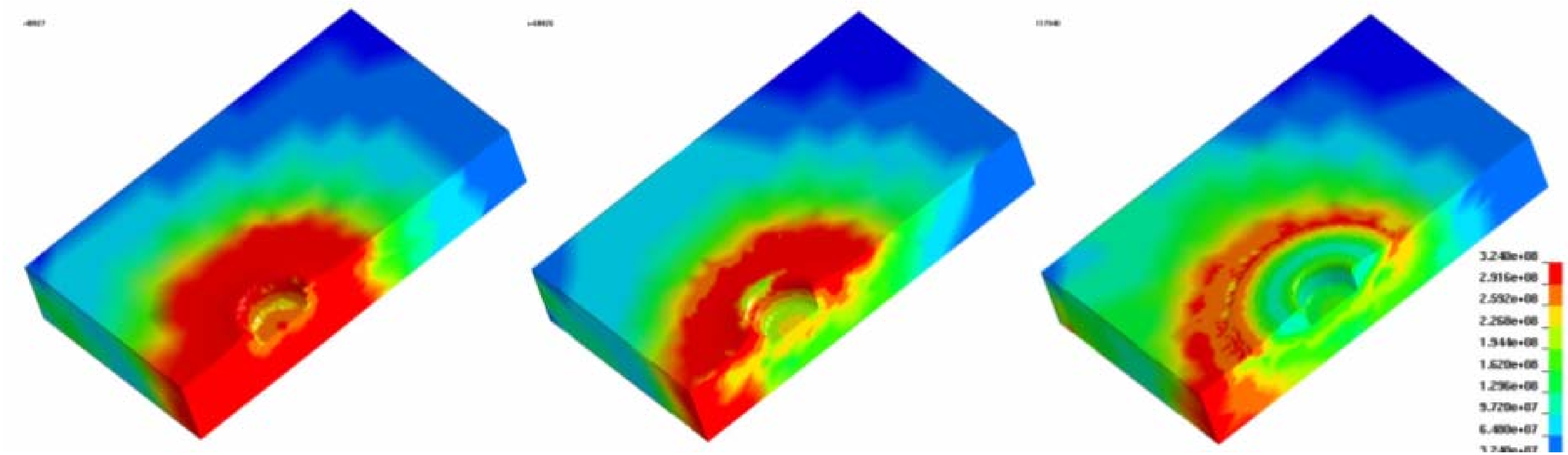

(a) *t=0.05s* (b) *t=0.15s* (c) *t=0.6s*

FSW Example (Cont.)

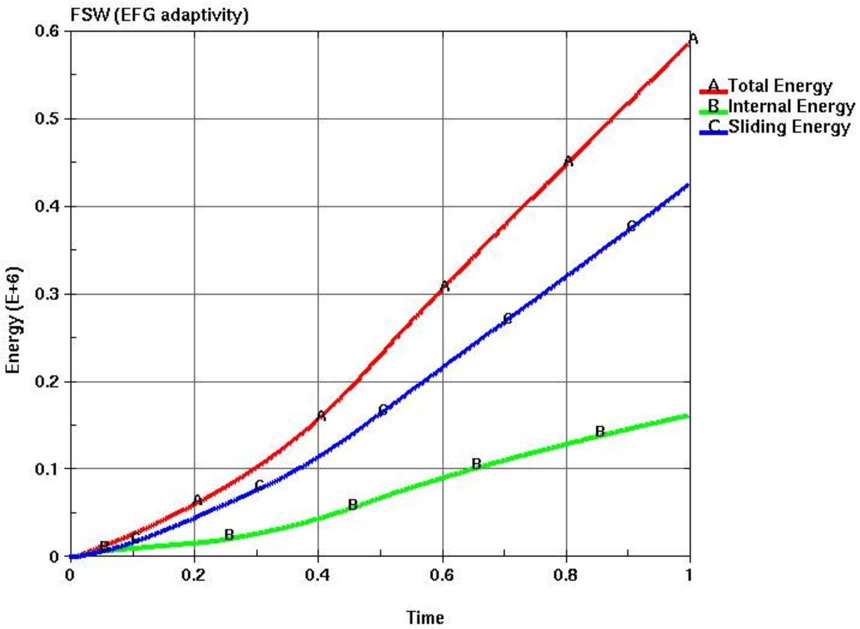

Energy

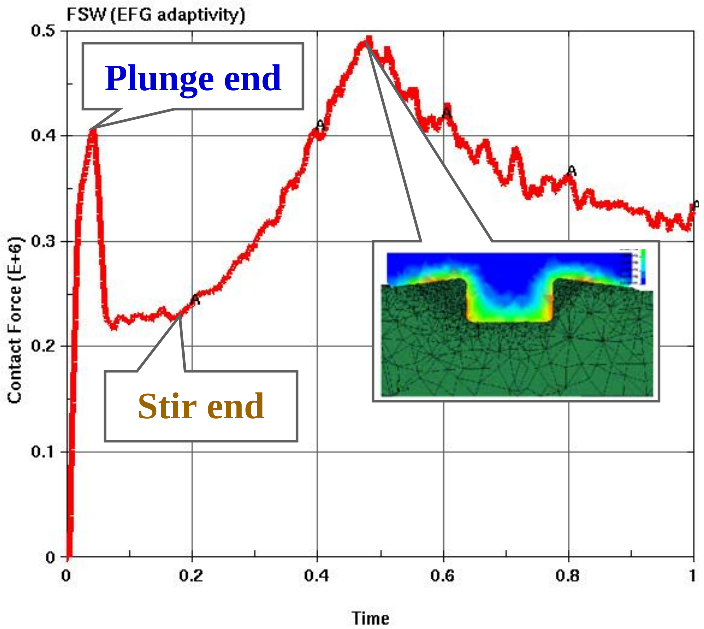

Contact Force

Part 2

Smoothed Particle Galerkin (SPG) Method
For Severe Deformation and Failure Analysis in Solid

Methods for Solid and Structural Analyses in LS-DYNA®

- *Rubber Materials*: FEM, EFG, MEFEM, SPG
- *Foam materials*: FEM, SPH, EFG, SPG
- *Metal materials*: FEM, SPH, EFG, MEFEM, Adaptive FEM and EFG, SPG
- *Quasi-brittle material fracture*: FEM, SPH, EFG, SPG, State-based Peridynamic method
- *E.O.S. materials and high speed applications*: ALE, SPH, SPG, State-based Peridynamic method
- *Shells*: FEM, EFG, SFEM
- *Soil*: ALE, SPH, EFG, SPG
- *Discrete materials*: Discrete element method (DEM)
- *Composites and Unit cell analysis*: FEM, EFG, SPG, Immersed Particle Galerkin method

Numerical Issues in Conventional Particle Analysis of Solids and Structures

- Lack of approximation consistency
  → Impose first-order reproducing condition
- Tension instability
  → Ensure material failure occurs before numerical fracture
- Material diffusion
  → Use higher-order integration scheme
- Presence of spurious or zero-energy modes
  → Need stabilization
- Difficulty in enforcing the boundary conditions
  → Special treatments (Convex approximation…)

3D Smoothed Particle Galerkin Method

FEM

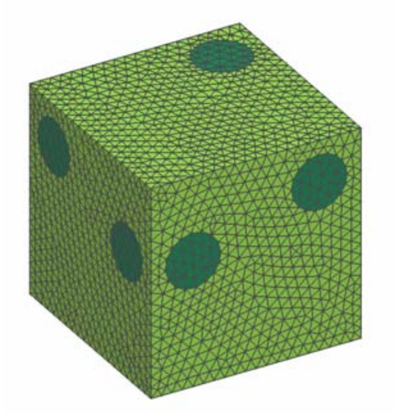

- Solid applications
- Read all FEM input formats
- A purely particle computation
- Handle severe deformation + failure

SPG

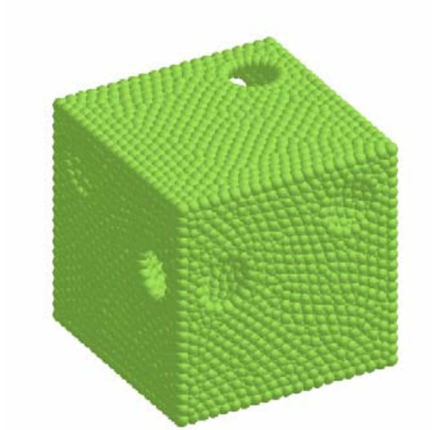

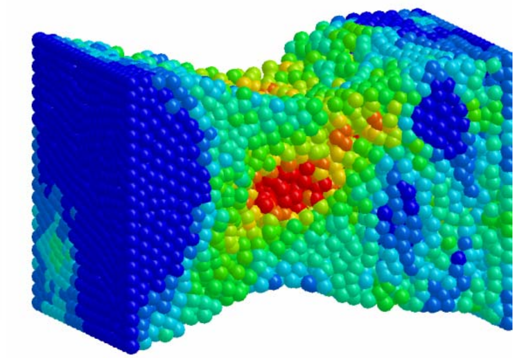

Main Features

Smoothed Particle Galerkin (SPG) Method

- Has explicit/implicit versions. Currently only explicit method implemented.
- A pure particle integration method without integration cell.
- Removes low-energy modes due to rank deficiency in nodal integration.
- Related to residual-based Galerkin meshfree method.
- Can be related to non-local or gradient types inelasticity.
- Without stabilization control parameters.
- Stability analysis via Variational Multi-scale analysis.
- First-order convergence in energy norm.
- Capable of providing a physical-based failure analysis.
- Ready to be released in this year.

Residual-based Stabilization Approach for Stabilized Meshfree Galerkin Nodal Integration

(Beissel and Belytschko 1996)

$$\pi_s(\boldsymbol{u},\boldsymbol{\lambda}) = \pi(\boldsymbol{u},\boldsymbol{\lambda}) + \frac{\alpha_s l_c^2}{E}\int_\Omega (\nabla\cdot\boldsymbol{\sigma}(\boldsymbol{u}) + \boldsymbol{b})^2 \, d\Omega$$

where

$$\pi(\boldsymbol{u},\boldsymbol{\lambda}) = \int_\Omega \left(\frac{1}{2}\boldsymbol{\varepsilon}(\boldsymbol{u}) : \boldsymbol{\sigma}(\boldsymbol{u}) - \boldsymbol{u}\cdot\boldsymbol{b}\right) d\Omega - \int_{\Gamma_t} \boldsymbol{u}\cdot\boldsymbol{t}\, d\Gamma + \int_{\Gamma_u} \boldsymbol{\lambda}\cdot\left(\boldsymbol{u} - \boldsymbol{u}^d\right) d\Gamma$$

α_s : Dimensionless stabilization parameter

l_c : a characteristic length scale of the discretization (or nodal arrangement)

Variation →

$$\delta\pi_s(\boldsymbol{u},\delta\boldsymbol{u},\boldsymbol{\lambda},\delta\boldsymbol{\lambda}) = 0$$

$$= \int_\Omega (\delta\boldsymbol{\varepsilon}(\boldsymbol{u}) : \boldsymbol{\sigma}(\boldsymbol{u}) - \delta\boldsymbol{u}\cdot\boldsymbol{b})\, d\Omega - \int_{\Gamma_t} \delta\boldsymbol{u}\cdot\boldsymbol{t}\, d\Gamma + \int_{\Gamma_u} \delta\boldsymbol{\lambda}\cdot\left(\boldsymbol{u} - \boldsymbol{u}^d\right) d\Gamma$$

$$+ \int_{\Gamma_u} \delta\boldsymbol{u}\cdot\boldsymbol{\lambda}\, d\Gamma + \boxed{\frac{2\alpha_s l_c^2}{E}\int_\Omega (\nabla\cdot\delta\boldsymbol{\sigma}(\boldsymbol{u}))\cdot(\nabla\cdot\boldsymbol{\sigma}(\boldsymbol{u}) + \boldsymbol{b})\, d\Omega}$$

Stabilization through Displacement Smoothing

(Wu et al. 2014)

- Smoothed Displacement field

$$\bar{\boldsymbol{u}}(\boldsymbol{X}) = \int_\Omega \underbrace{\tilde{\Psi}(\boldsymbol{Y};\boldsymbol{X})}_{\text{Smoothing function}} \underbrace{\hat{\boldsymbol{u}}(\boldsymbol{Y})}_{\text{Physical displacement}} d\Omega$$

Taylor expansion

$$\hat{\boldsymbol{u}}(\boldsymbol{Y}) = \hat{\boldsymbol{u}}(\boldsymbol{X}) + \nabla\hat{\boldsymbol{u}}(\boldsymbol{X})\cdot(\boldsymbol{Y}-\boldsymbol{X}) + \frac{1}{2!}\nabla^{(2)}\hat{\boldsymbol{u}}(\boldsymbol{X})\cdot^{(2)}(\boldsymbol{Y}-\boldsymbol{X})^{(2)} + \frac{1}{3!}\nabla^{(3)}\hat{\boldsymbol{u}}(\boldsymbol{X})\cdot^{(3)}(\boldsymbol{Y}-\boldsymbol{X})^{(3)} + \cdots$$

$$\begin{aligned}\bar{\boldsymbol{u}}(\boldsymbol{X}) &= \int_\Omega \tilde{\Psi}(\boldsymbol{Y};\boldsymbol{X})\hat{\boldsymbol{u}}(\boldsymbol{X})d\Omega + \int_\Omega \tilde{\Psi}(\boldsymbol{Y};\boldsymbol{X})\nabla\hat{\boldsymbol{u}}(\boldsymbol{X})\cdot(\boldsymbol{Y}-\boldsymbol{X})d\Omega \\ &+ \frac{1}{2!}\int_\Omega \tilde{\Psi}(\boldsymbol{Y};\boldsymbol{X})\nabla^{(2)}\hat{\boldsymbol{u}}(\boldsymbol{X})\cdot^{(2)}(\boldsymbol{Y}-\boldsymbol{X})^{(2)}d\Omega \\ &+ \frac{1}{3!}\int_\Omega \tilde{\Psi}(\boldsymbol{Y};\boldsymbol{X})\nabla^{(3)}\hat{\boldsymbol{u}}(\boldsymbol{X})\cdot^{(3)}(\boldsymbol{Y}-\boldsymbol{X})^{(3)}d\Omega + O(\|\boldsymbol{Y}-\boldsymbol{X}\|)^{(4)}\end{aligned}$$

Neglect high-order terms

$$\begin{aligned}\bar{\boldsymbol{u}}(\boldsymbol{X}) &\approx \int_\Omega \tilde{\Psi}(\boldsymbol{Y};\boldsymbol{X})\hat{\boldsymbol{u}}(\boldsymbol{X})d\Omega + \int_\Omega \tilde{\Psi}(\boldsymbol{Y};\boldsymbol{X})\nabla\hat{\boldsymbol{u}}(\boldsymbol{X})\cdot(\boldsymbol{Y}-\boldsymbol{X})d\Omega \\ &+ \frac{1}{2!}\int_\Omega \tilde{\Psi}(\boldsymbol{Y};\boldsymbol{X})\nabla^{(2)}\hat{\boldsymbol{u}}(\boldsymbol{X})\cdot^{(2)}(\boldsymbol{Y}-\boldsymbol{X})^{(2)}d\Omega \\ &= \hat{\boldsymbol{u}}(\boldsymbol{X})\int_\Omega \tilde{\Psi}(\boldsymbol{Y};\boldsymbol{X})d\Omega + \nabla\hat{\boldsymbol{u}}(\boldsymbol{X})\underbrace{\left(\int_\Omega \tilde{\Psi}(\boldsymbol{Y};\boldsymbol{X})(\boldsymbol{Y})d\Omega - \boldsymbol{X}\int_\Omega \tilde{\Psi}(\boldsymbol{Y};\boldsymbol{X})d\Omega\right)}_{0} \\ &+ \nabla^{(2)}\hat{\boldsymbol{u}}(\boldsymbol{X})\cdot^{(2)}\left(\frac{1}{2!}\int_\Omega \tilde{\Psi}(\boldsymbol{Y};\boldsymbol{X})(\boldsymbol{Y}-\boldsymbol{X})^{(2)}d\Omega\right) \\ &= \hat{\boldsymbol{u}}(\boldsymbol{X})\int_\Omega \tilde{\Psi}(\boldsymbol{Y};\boldsymbol{X})d\Omega + \nabla^{(2)}\hat{\boldsymbol{u}}(\boldsymbol{X})\cdot^{(2)}\left(\frac{1}{2!}\int_\Omega \tilde{\Psi}(\boldsymbol{Y};\boldsymbol{X})(\boldsymbol{Y}-\boldsymbol{X})^{(2)}d\Omega\right) \\ &= \hat{\boldsymbol{u}}(\boldsymbol{X}) + \nabla^{(2)}\hat{\boldsymbol{u}}(\boldsymbol{X})\cdot^{(2)}\boldsymbol{\eta}(\boldsymbol{X})\end{aligned}$$

Modified Meshfree Galerkin Principle

- Variational formulation

$$a^h(\hat{\boldsymbol{u}},\delta\hat{\boldsymbol{u}}) = l(\delta\hat{\boldsymbol{u}}) \;\; \forall\, \delta\hat{\boldsymbol{u}} \in \boldsymbol{V}^h$$

$$a^h(\hat{\boldsymbol{u}},\delta\hat{\boldsymbol{u}}) = \int_\Omega \delta\left(\nabla^s\hat{\boldsymbol{u}}\right):\boldsymbol{C}:\left(\nabla^s\hat{\boldsymbol{u}}\right)d\Omega + \int_\Omega \delta\left(\overline{\nabla}^{(2)}\hat{\boldsymbol{u}}\right):\boldsymbol{C}:\left(\overline{\nabla}^{(2)}\hat{\boldsymbol{u}}\right)d\Omega$$

$$= a^h_{stan}(\hat{\boldsymbol{u}},\delta\hat{\boldsymbol{u}}) + a^h_{stab}(\hat{\boldsymbol{u}},\delta\hat{\boldsymbol{u}})$$

$$a^h_{stab}(\hat{\boldsymbol{u}},\delta\hat{\boldsymbol{u}}) = \int_\Omega \delta\left(\overline{\nabla}^{(2)}\hat{\boldsymbol{u}}\right):\boldsymbol{C}:\left(\overline{\nabla}^{(2)}\hat{\boldsymbol{u}}\right)d\Omega \Longleftrightarrow 2\alpha_s l_c^2 \int_\Omega \delta\left(\nabla^{(2)}\hat{\boldsymbol{u}}\right):\boldsymbol{C'}:\left(\nabla^{(2)}\hat{\boldsymbol{u}}\right)d\Omega$$

Residual-based stabilization method

$$\overline{\nabla}^{(2)}\hat{\boldsymbol{u}} = \frac{1}{2}\left(\nabla\boldsymbol{\eta}:\hat{\boldsymbol{u}}\nabla^{(2)} + \left(\nabla\boldsymbol{\eta}:\hat{\boldsymbol{u}}\nabla^{(2)}\right)^T\right)$$

Smoothed second-order gradient

$$l(\delta\hat{\boldsymbol{u}}) = \int_\Omega \delta\hat{\boldsymbol{u}}\cdot\boldsymbol{f}d\Omega + \int_{\Gamma_N}\delta\hat{\boldsymbol{u}}\cdot\boldsymbol{t}d\Gamma - \int_\Omega\left(\delta\nabla^{(2)}\hat{\boldsymbol{u}}:\boldsymbol{\eta}\right)\cdot\boldsymbol{f}d\Omega$$

$$\boldsymbol{\eta}(\boldsymbol{X}) = \frac{1}{2!}\int_\Omega \widetilde{\Psi}(\boldsymbol{Y};\boldsymbol{X})(\boldsymbol{Y}-\boldsymbol{X})^{(2)}d\Omega$$: Position dependent stabilization coefficient → $a^h_{stab} \propto l_c^2$

$\nabla^{(n)}$ denotes the nth order gradient operator

$\cdot^{(n)}$ denotes the nth order inner product.

The symbol $(\xi)^{(n)}$ designates the n factor dyadic product $(\xi)(\xi)\cdots(\xi)$ for vector ξ

Nonlinear SPG Implementation

Implicit formulation $\Delta\delta\Pi = \int_{\Omega_x} \delta\varepsilon_{ij} C_{ijkl} \Delta\varepsilon_{kl} d\Omega + \int_{\Omega_x} \delta u_{i,j} T_{ijkl} \Delta u_{k,l} d\Omega - \int_{\Omega_x} \delta u_i \Delta f_i d\Omega - \int_{\Gamma_N} \delta u_i \Delta t_i d\Gamma$

$$\Longrightarrow \delta\tilde{\boldsymbol{U}}^T \boldsymbol{K}_{n+1}^v \left(\Delta\tilde{\boldsymbol{U}}\right)_{n+1}^{v+1} = \delta\tilde{\boldsymbol{U}}^T \boldsymbol{R}_{n+1}^v$$

$$\Longrightarrow \tilde{\boldsymbol{U}} = \boldsymbol{A}^{-1}\bar{\boldsymbol{U}}$$

$$\boldsymbol{A}_{IJ} = \phi_J\left(\boldsymbol{X}_I\right)\boldsymbol{I} = \sum_{K=1}^{NP} \Psi_K\left(\boldsymbol{X}_I\right)\Psi_J\left(\boldsymbol{X}_K\right)\boldsymbol{I}$$

$$\boldsymbol{A}^{-T} \boldsymbol{K}_{n+1}^v \boldsymbol{A}^{-1} \left(\Delta\bar{\boldsymbol{U}}\right)_{n+1}^{v+1} = \boldsymbol{A}^{-T} \boldsymbol{R}_{n+1}^v$$

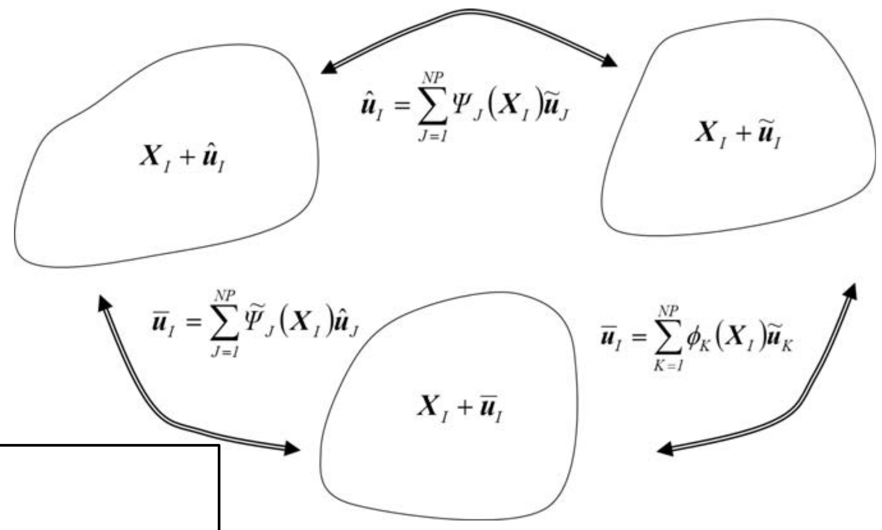

Explicit dynamic formulation

$$\Longrightarrow \boldsymbol{A}^{-T} \boldsymbol{M} \boldsymbol{A}^{-1} \ddot{\bar{\boldsymbol{U}}} = \boldsymbol{A}^{-T}\left(\boldsymbol{f}^{ext} - \boldsymbol{f}^{\text{int}}\right)$$

$$\Longrightarrow \bar{\boldsymbol{M}} \ddot{\bar{\boldsymbol{U}}} = \boldsymbol{A}^{-T}\left(\boldsymbol{f}^{ext} - \boldsymbol{f}^{\text{int}}\right)$$

$$\bar{\boldsymbol{M}}_I^{RS} = \sum_J^{NP} \bar{\boldsymbol{M}}_{IJ} = \sum_J^{NP} \boldsymbol{A}_{IK}^{-T} \boldsymbol{M}_{KM} \boldsymbol{A}_{ML}^{-1}$$

$$\frac{d\rho_I}{dt} = -\rho_I \nabla \cdot \left(\dot{\tilde{\boldsymbol{u}}}_I\right) = -\rho_I \sum_{J=1}^{NP} \dot{\tilde{\boldsymbol{u}}}_J \cdot \Psi_{J,\boldsymbol{x}}\left(\boldsymbol{x}_I\right)$$

Explicit formulation currently implemented in LS-DYNA©

Updated Lagrangain /Eulerian Kernels

$$\Psi^{-}_{I,i}\left(\boldsymbol{x}^{k+1}\right)=\frac{\partial \Psi_I^{-}\left(\boldsymbol{x}^{k+1}\right)}{\partial x_i^{k+1}}=\frac{\partial \Psi_I^{-}\left(\boldsymbol{x}^{k+1}\right)}{\partial x_j^{k}}\frac{\partial x_j^{k}}{\partial x_j^{k+1}}=\frac{\partial \Psi_I^{-}}{\partial x_j^{k}}f_{ji}^{k-1}$$

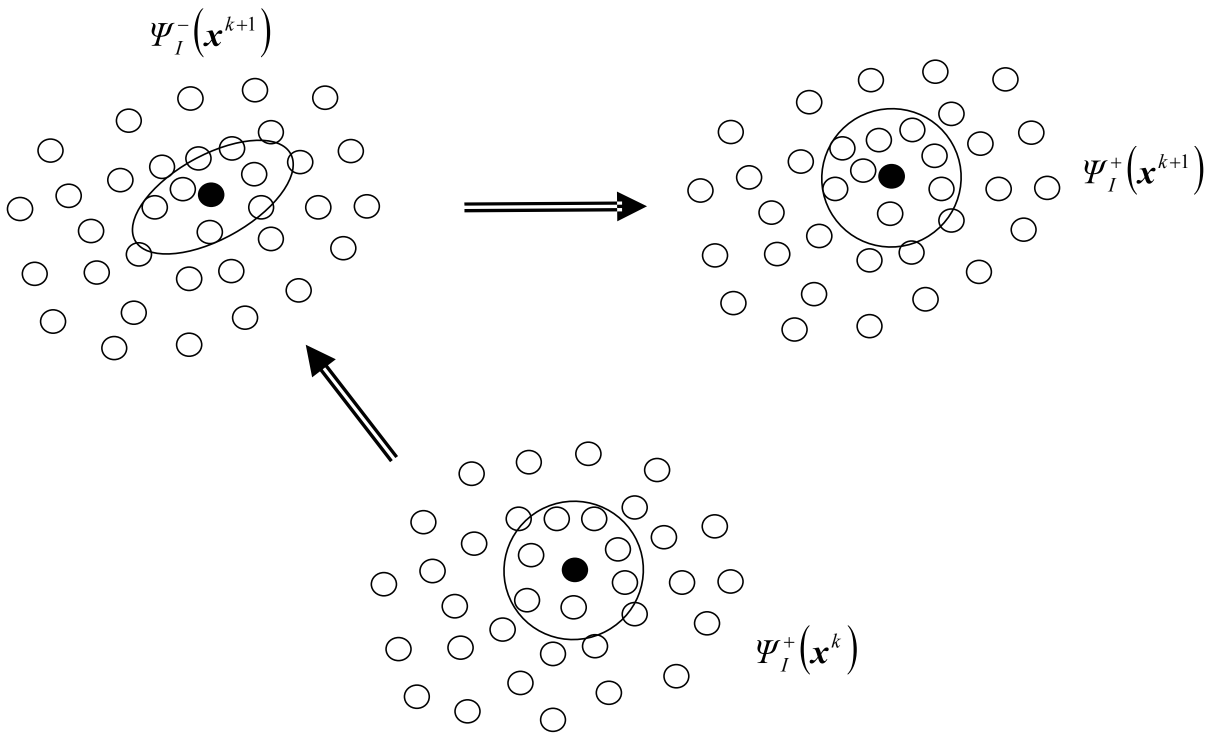

Consistency + Stability = Convergence

First-order rate of convergence in energy norm !

Material fracture v.s. Numerical fracture

Reference configuration

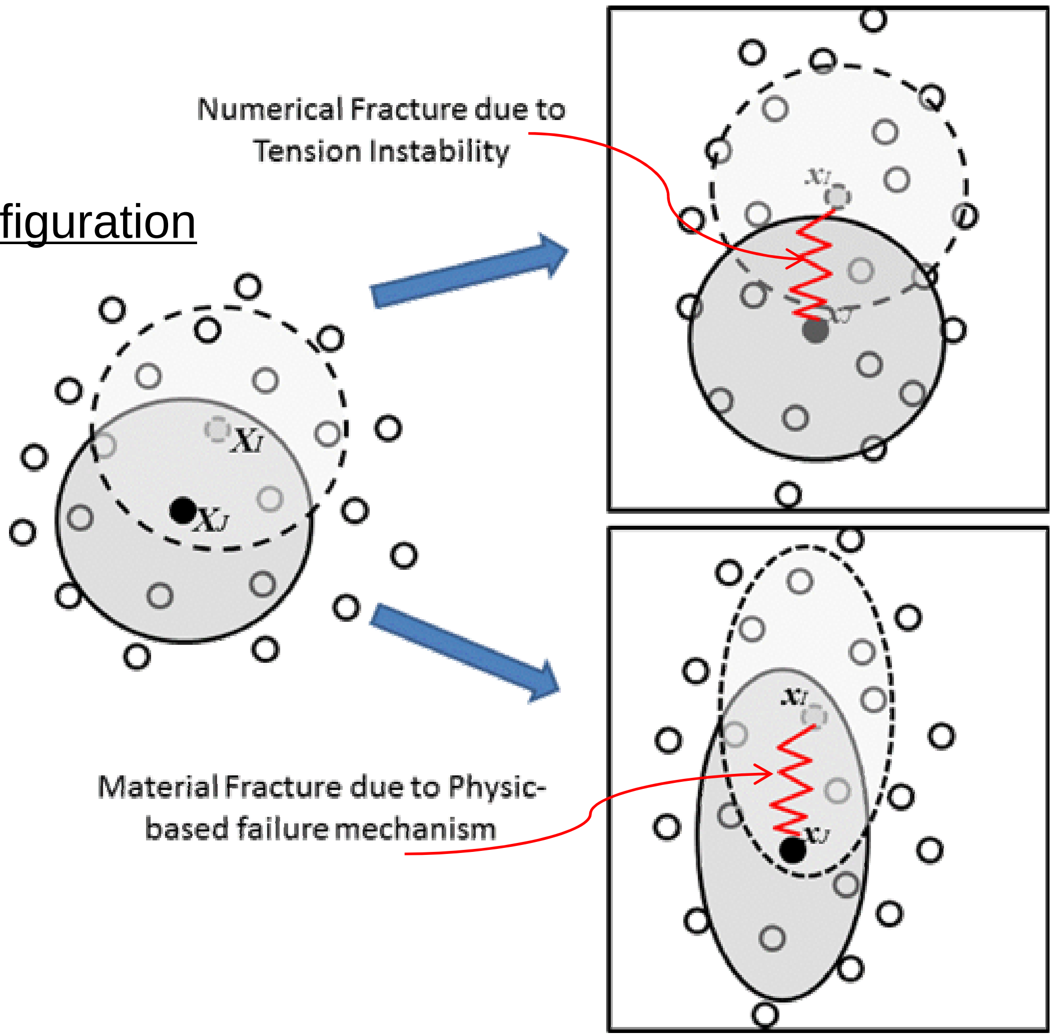

Deformed configuration

physical material fracture before numerical fracture ⟶ Enlarge numerical support !

Keyword Input Format

*SECTION_SOLID_SPG

Card1	1	2	3	4	5	6	7	8
Variable	SECID	ELFORM	AET					
Type	I	47	I					
Default								

Card2	1	2	3	4	5	6	7	8
Variable	DX	DY	DZ	ISPLINE	KERNEL	LSCALE	SMSTEP	SUKTIME
Type	F	F	F	I	I	F	I	F
Default	1.5	1.5	1.5	0	4		15	
Card3	1	2	3	4	5	6	7	8
Variable	IDAM	FS						
Type	I	F						
Default	0							

- Read 3D solid finite element (Tet/Hex) model as input

Keyword Input Format

VARIABLE	DESCRIPTION
SECID	Section ID.
ELFORM	Element formulation options. Set to 47 to active SPG method.
DX, DY, DZ	Normalized dilation parameters of the kernel functions in X, Y and Z directions.
ISPLINE	Option for kernel functions. EQ.0: Cubic spline function (default). EQ.1: Quadratic spline function. EQ.2: Cubic spline function with circular shape.
KERNEL	Type of kernel approximation. EQ.0: updated Lagrangian kernel. [Rubber-like material] EQ.1: Eulerian kernel. [EOS, Solid fluid] EQ.2: Semi-pseudo Lagrangian kernel. [Brittle, Semi-brittle] **EQ.3: pseudo Lagrangian kernel. (default) [Brittle, Semi-brittle, Ductile]**
LSCALE	Length scale for displacement regularization.
SMSTEP	Interval of time steps to conduct displacement regularization.
SUKTIME	(Reserved for time interval to update kernel information)
IDAM	Damage option. **EQ.0: Continuum Mechanical Damage** EQ.1: Phenomenological Strain Damage **EQ.2: Maximum principle Strain Damage**
FS	Failure strain if IDAM=1.

3D Prandtl's nonlinear punch problem

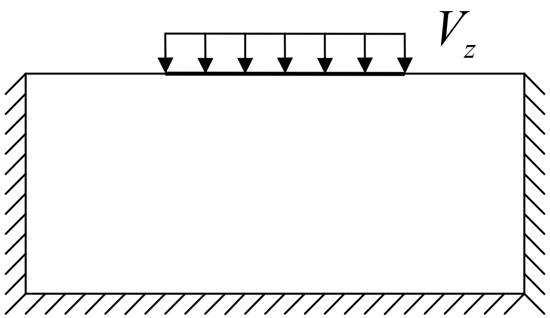

Dimension: 4x2x1

Particles: 21x11x6

Elastic material: E=6.9x10^4 , ν=0.3 V_z=2

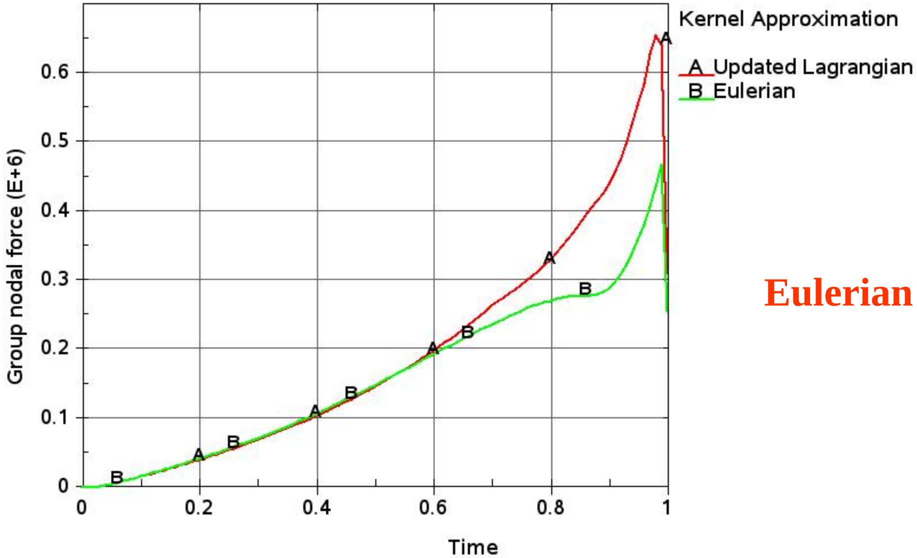

Updated

Lagrangian kernel

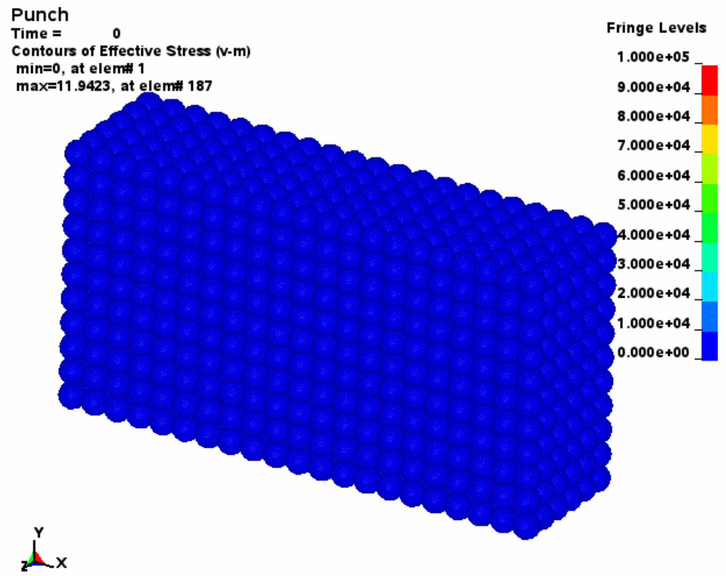

Eulerian kernel

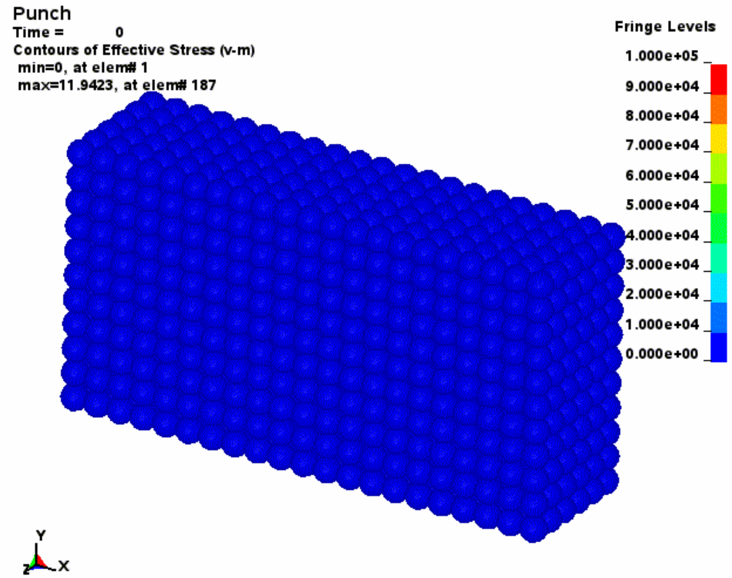

3D Prandtl's nonlinear punch problem

Updated Lagrangian

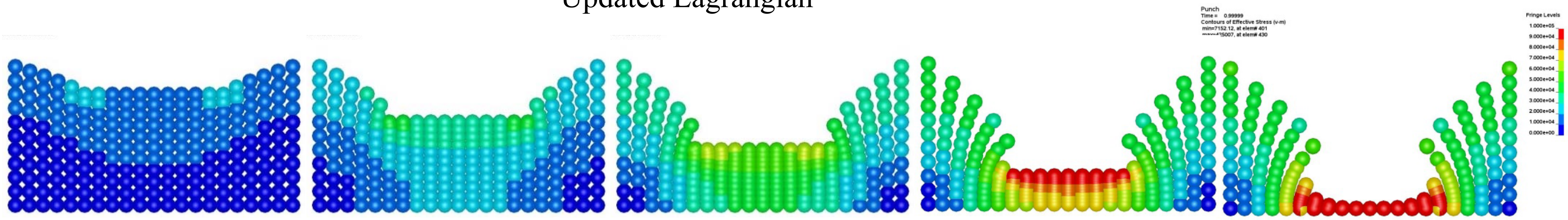

Fixed $\Delta t = 3.0 \times 10^{-5}$

t=0.2 0.4 0.6 0.8 1.0

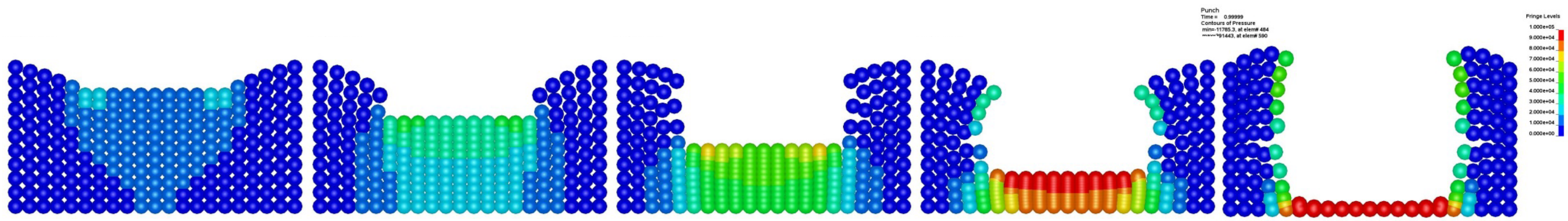

Eulerian

Taylor Bar Impact

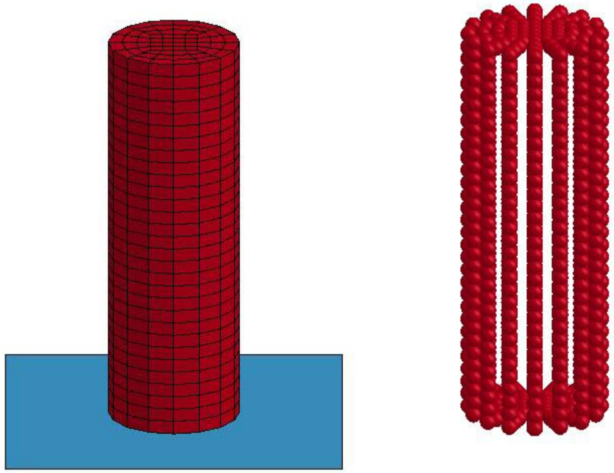

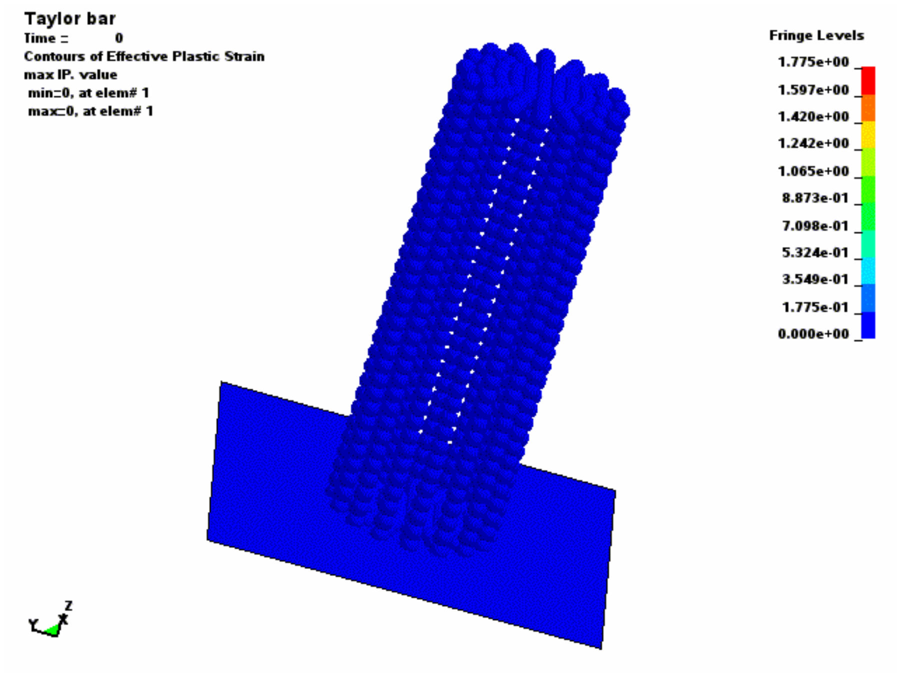

R=3.91 mm

H=23.46 mm

$\rho_0 = 2.7 \times 10^{-6}$ kg/mm^3

E=78.2GPa

v=0.3

$\sigma_y = 0.29(1+125e^p)^{0.1}$

V_0=373 mm/ms

Particles: 2263

DX=DY=DZ=1.4   SMSTEP=25

Final H=18.07mm

Exp. H=16.51mm

Taylor Bar Impact

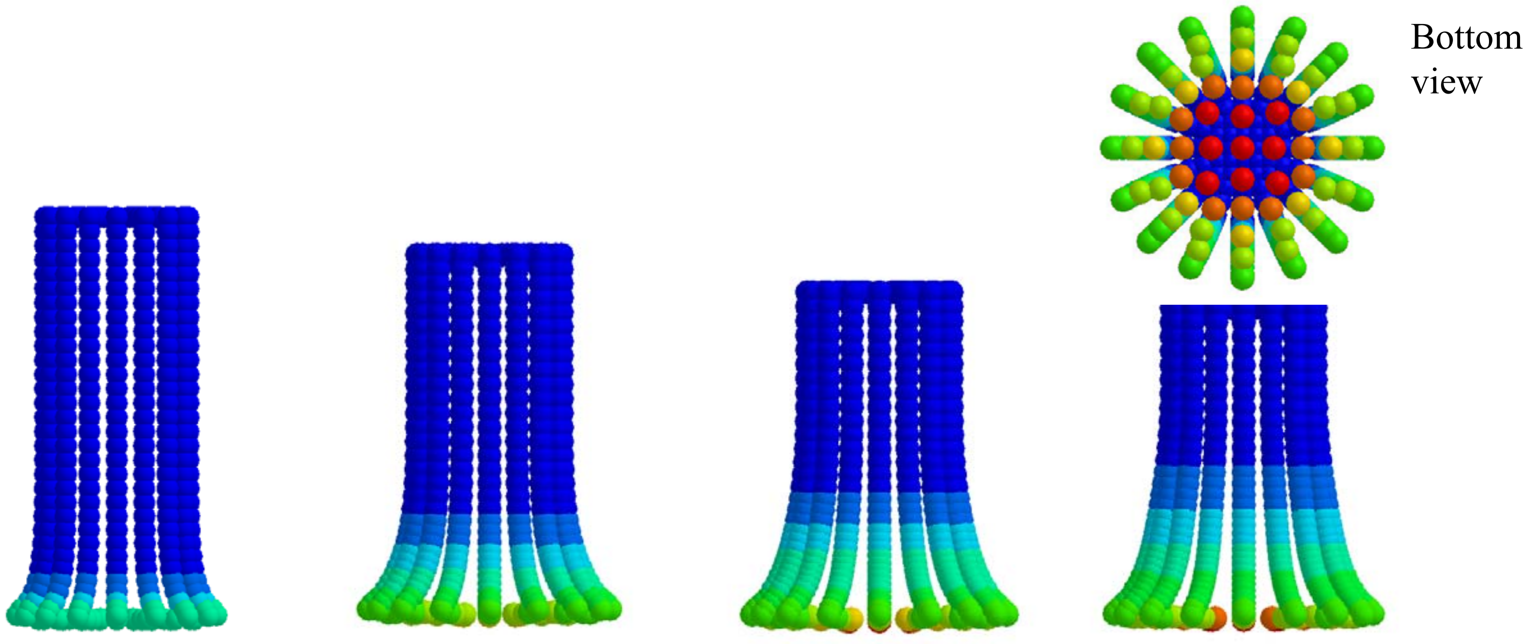

t=0.004	0.012	0.020	0.028
$\Delta t=1.76\times10^{-5}$	1.72×10^{-5}	1.66×10^{-5}	1.66×10^{-5}

Progressive deformation with effective plastic strain contour

Penetration Simulation (Ductile)

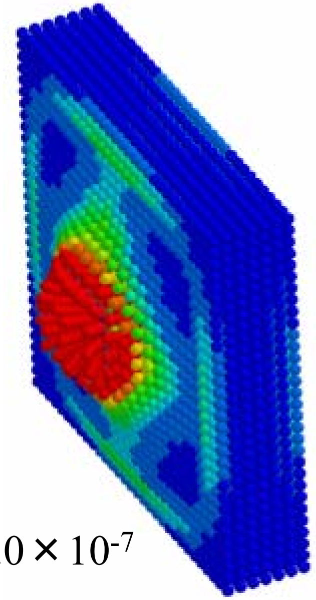

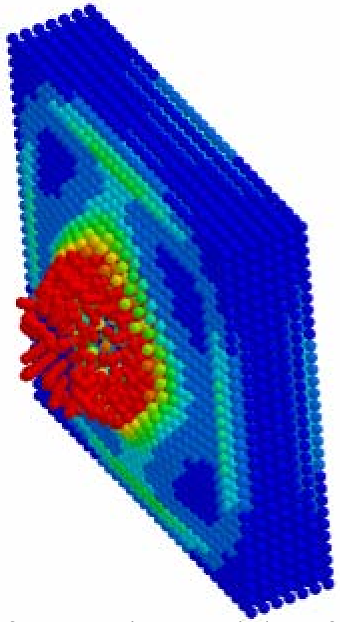

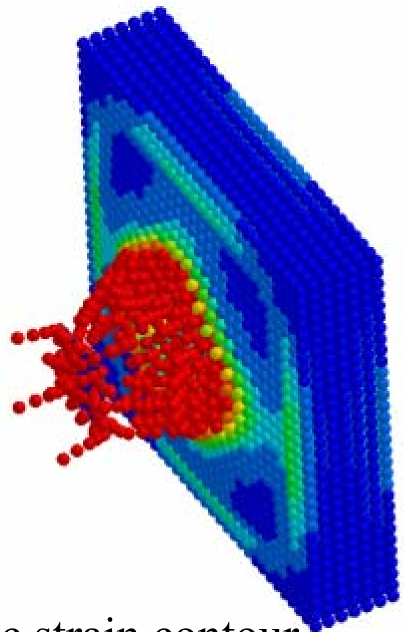

Aluminum

Fixed $\Delta t=1.0\times 10^{-7}$

Damage-mechanics 0.05~0.5

Progressive deformation with effective plastic strain contour

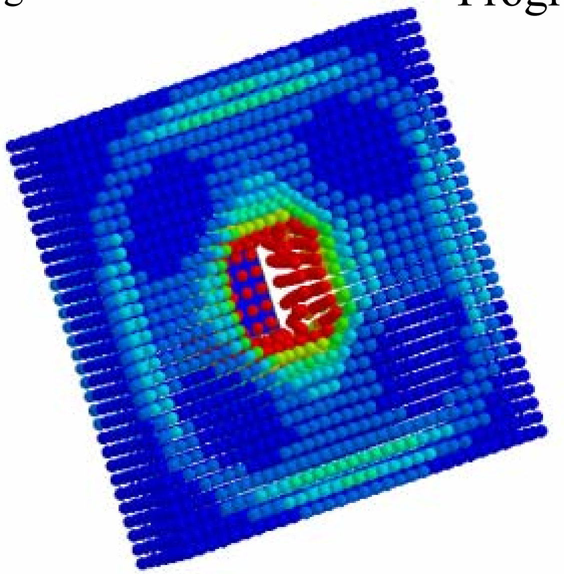

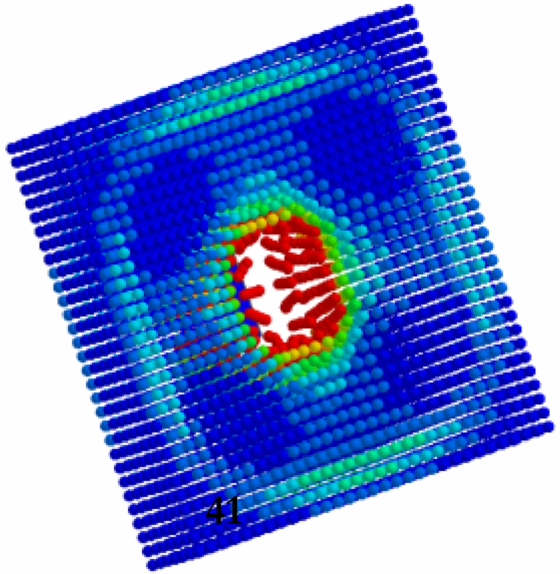

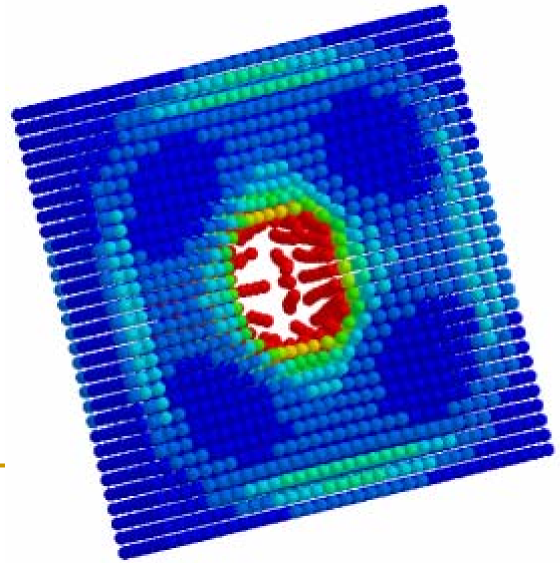

Penetration Simulation (Brittle)

Progressive deformation with damage contour

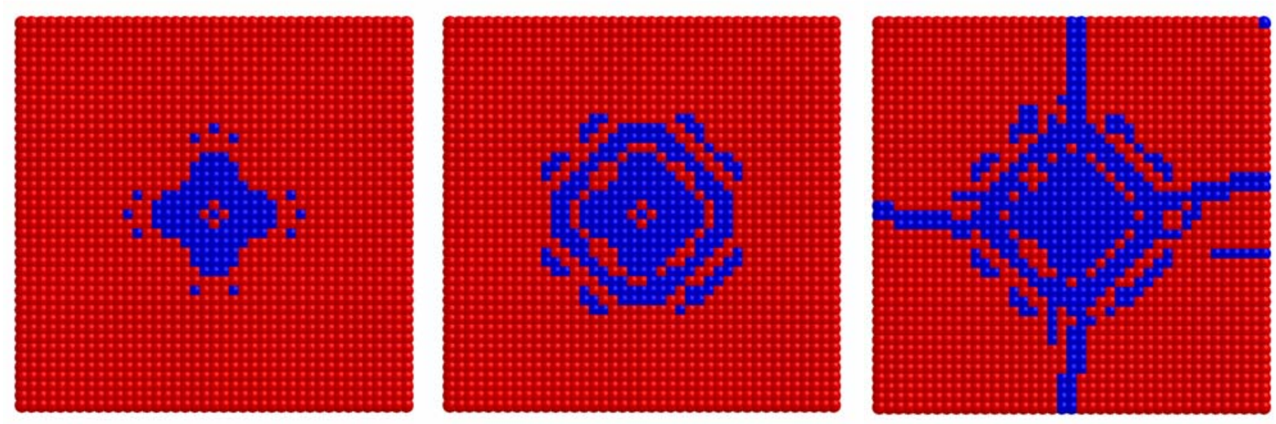

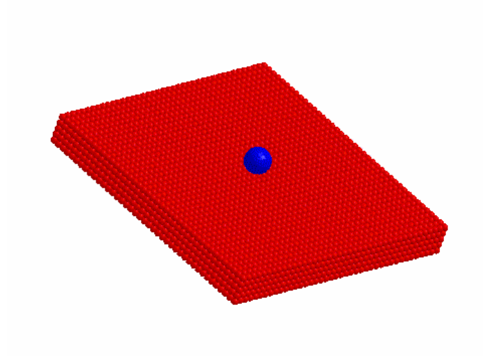

Top view

Velocity field

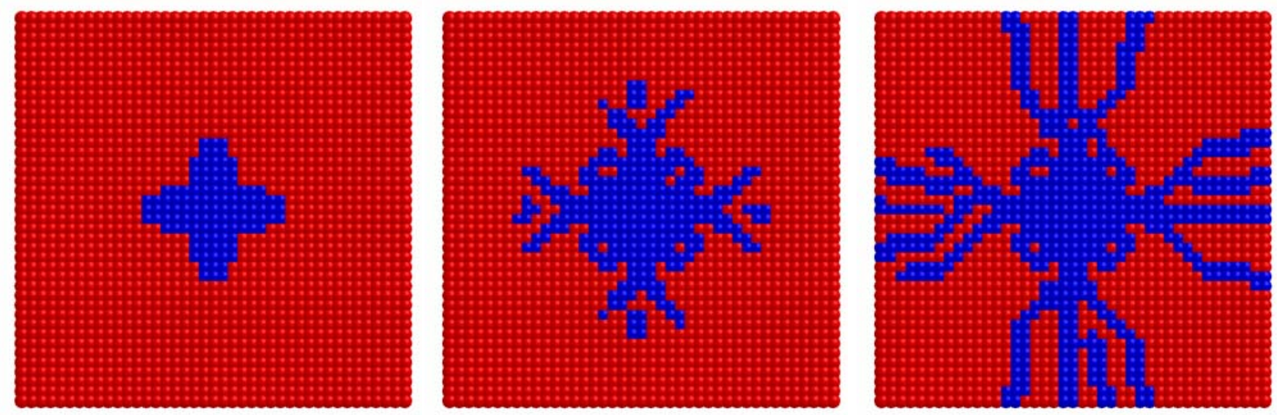

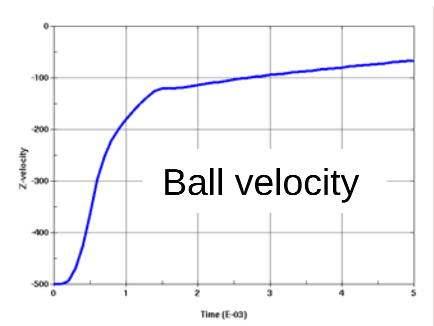

Bottom view

Metal Cutting Analysis

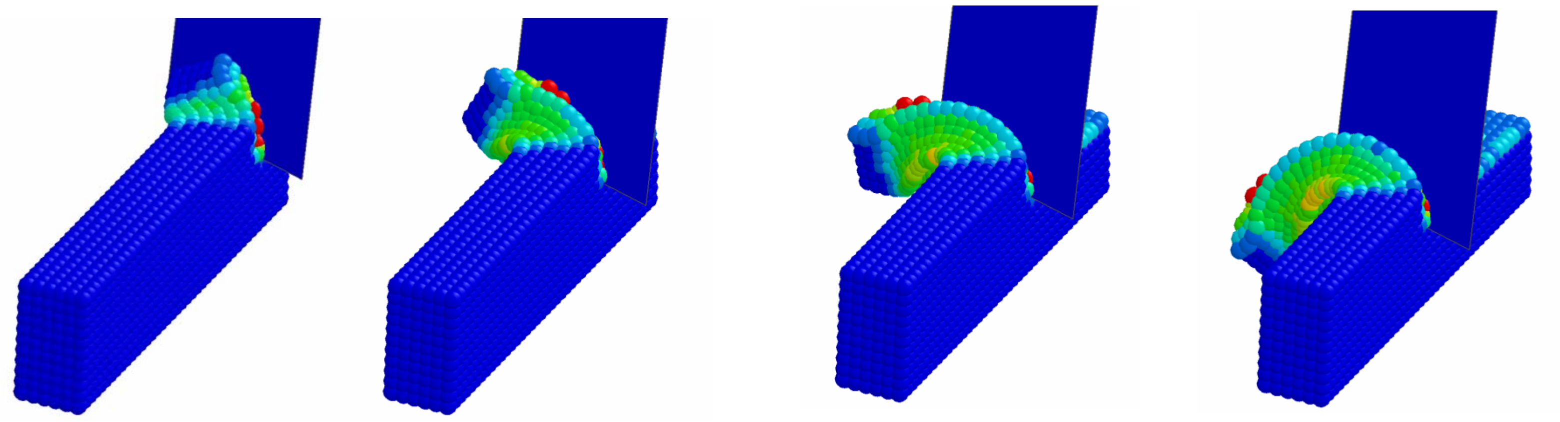

Aluminum
$\rho_0 = 2.7 \times 10^{-6}$ kg/mm^3
E=78.2GPa
v=0.3
$\sigma_y = 0.29(1+125e^p)^{0.1}$

Strain-based failure criteria $\varepsilon^{fail} = 0.5$

Cutting Speed = 10 m/s
Fixed $\Delta t = 3.0 \times 10^{-5}$

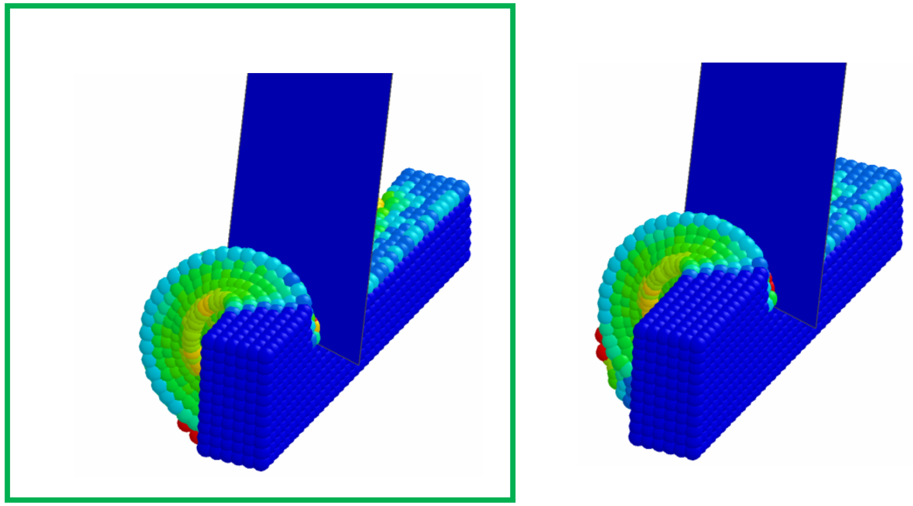

Metal shearing analysis

5% clearance

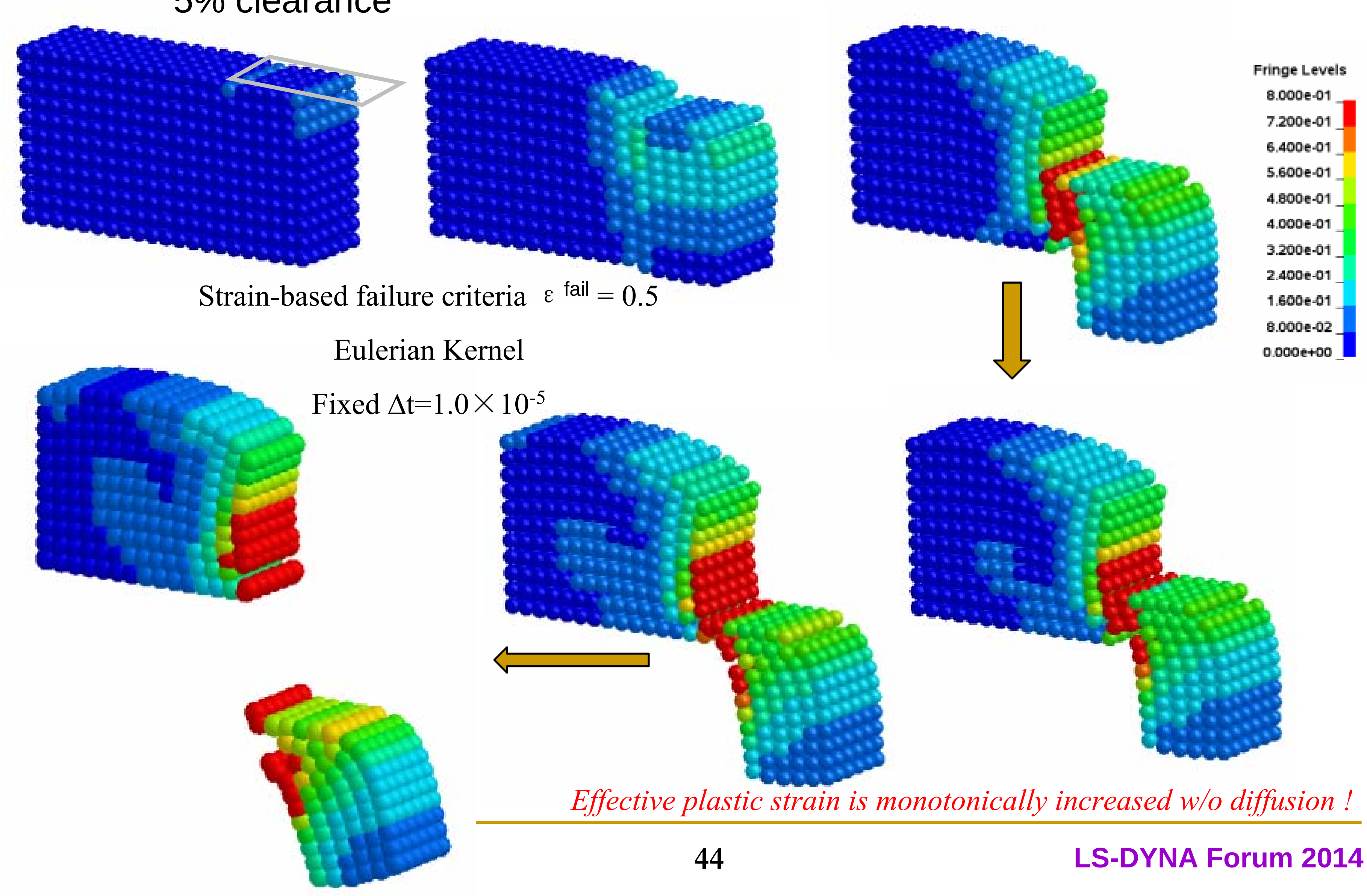

Strain-based failure criteria $\varepsilon^{fail} = 0.5$

Eulerian Kernel

Fixed $\Delta t=1.0 \times 10^{-5}$

Effective plastic strain is monotonically increased w/o diffusion !

Metal shearing analysis

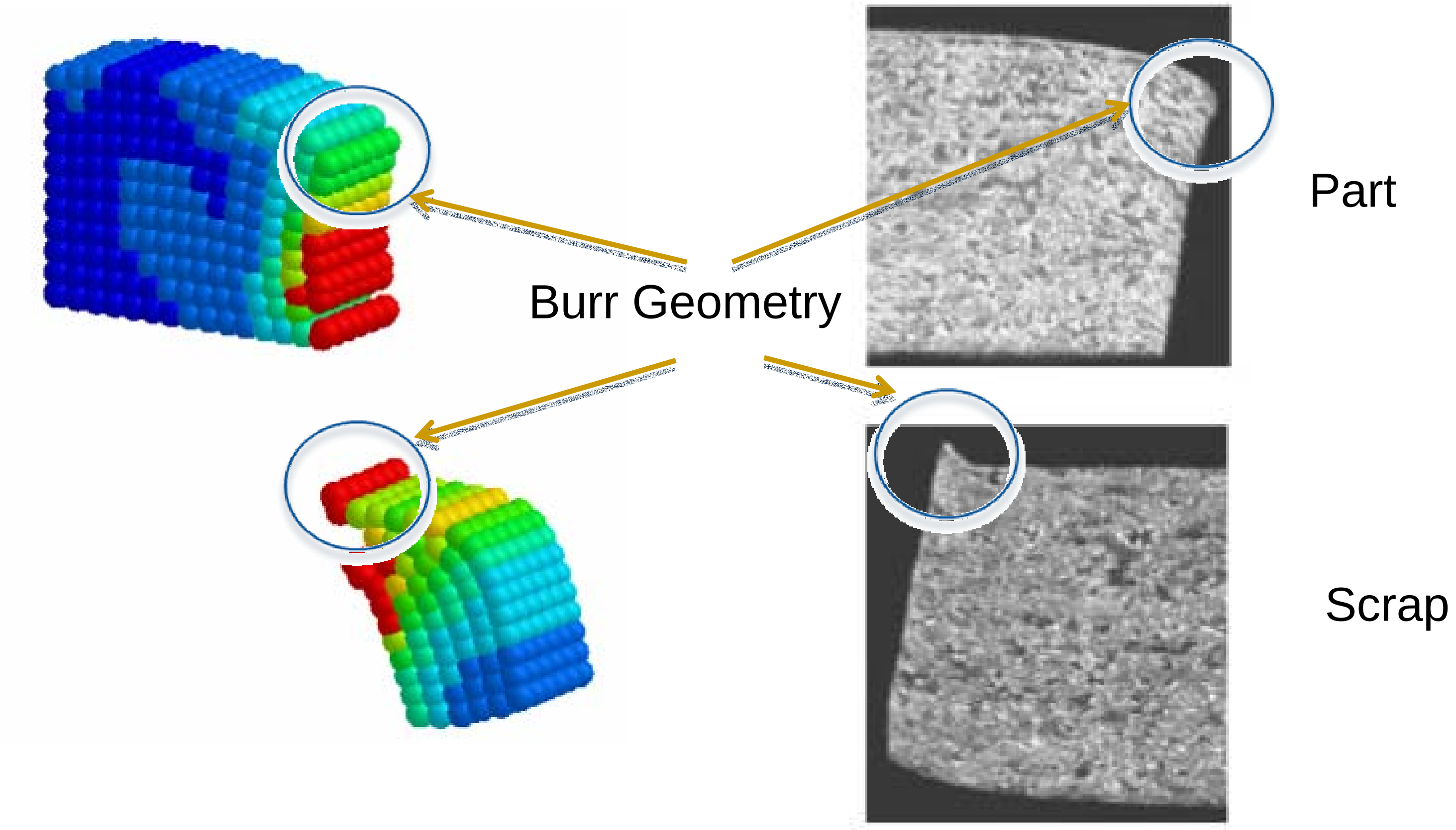

SPG simulation Experiment

Major applications in blanking, bolt/rivet shearing, AHSS trimming … !

Partical reinforced rubber material

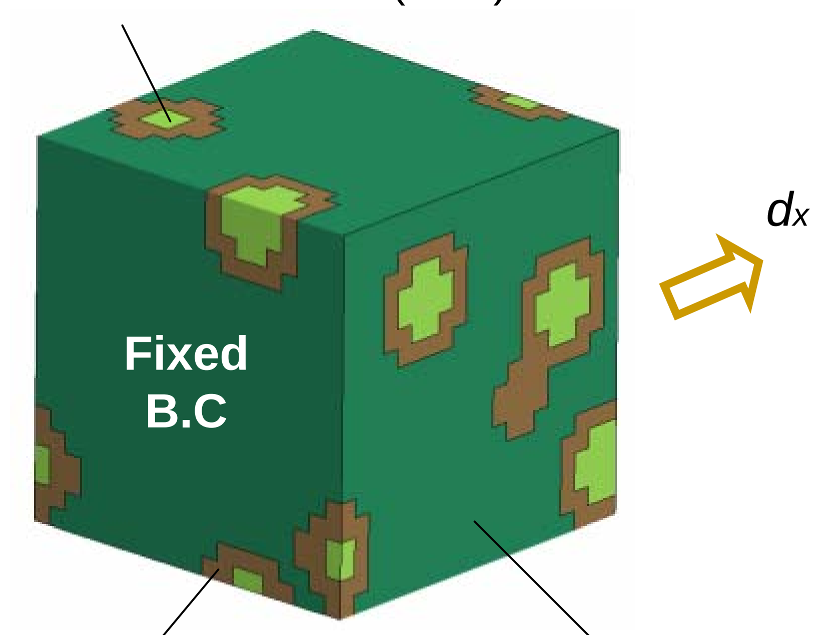

Base-Matrix Rubber:

EFG (implicit)

SPG (explicit)

- MAT_HYPERELASTIC_RUBBER
- Implicit / Explicit
- EFG
- SPG (Lagrangian / Eulerian)
- Stretching up to 20%
- Prescribed displacement d_x:

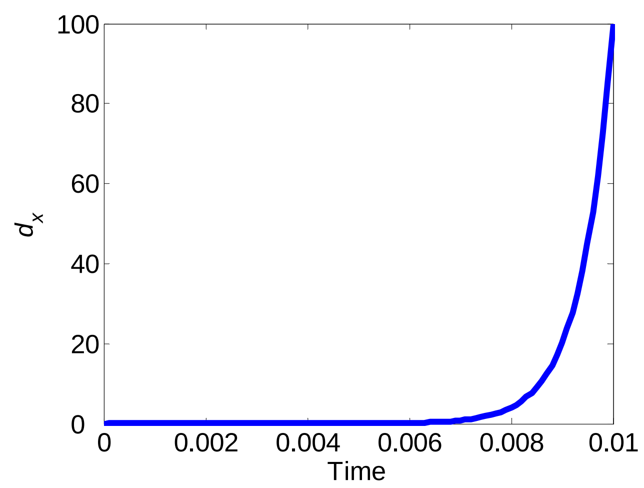

Partical reinforced rubber material

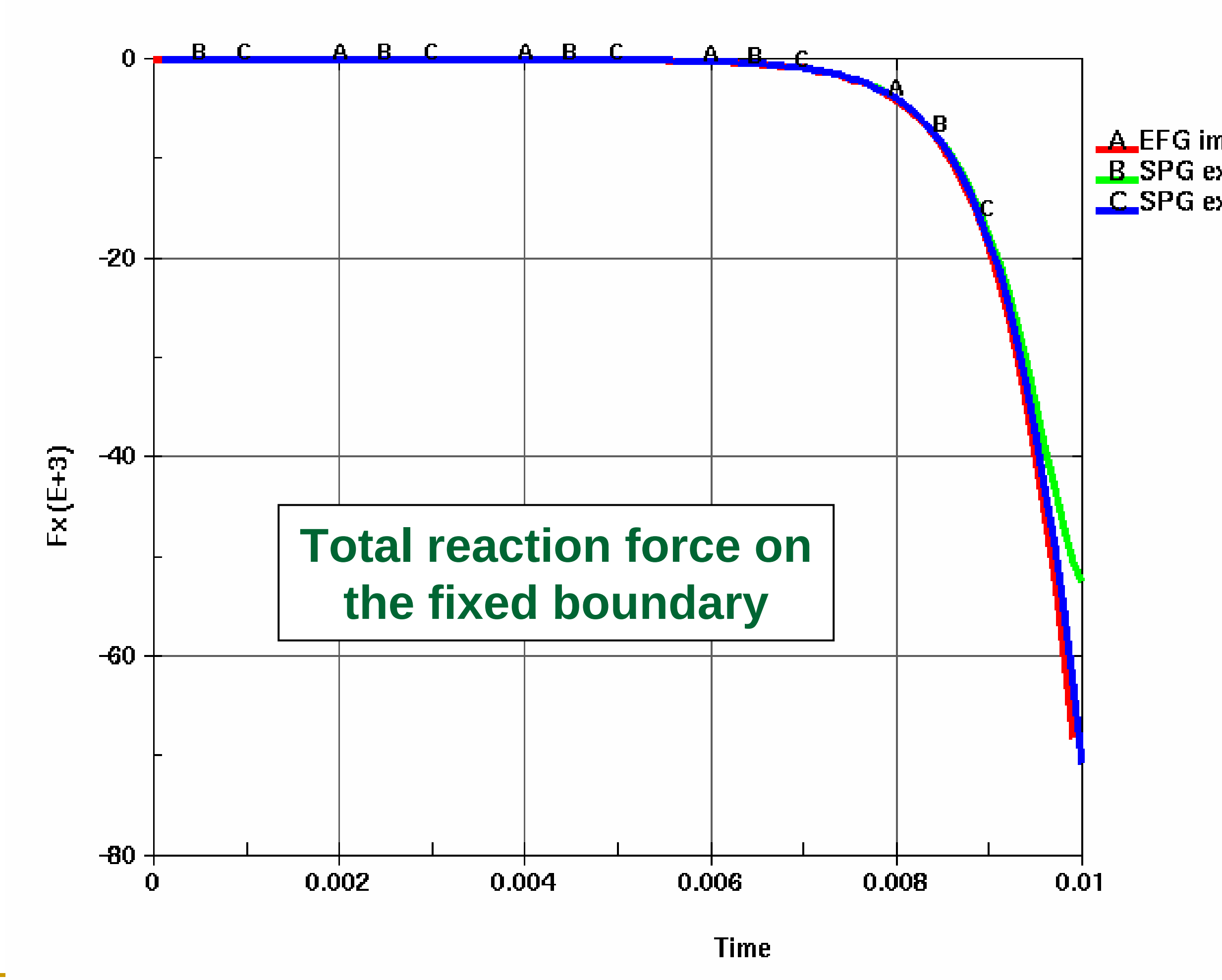

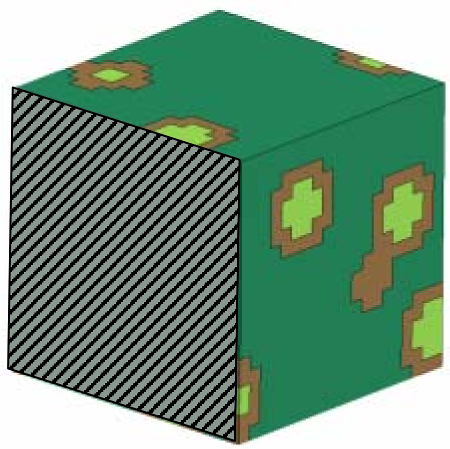

Partical reinforced rubber material

1st Principle Stress Contour

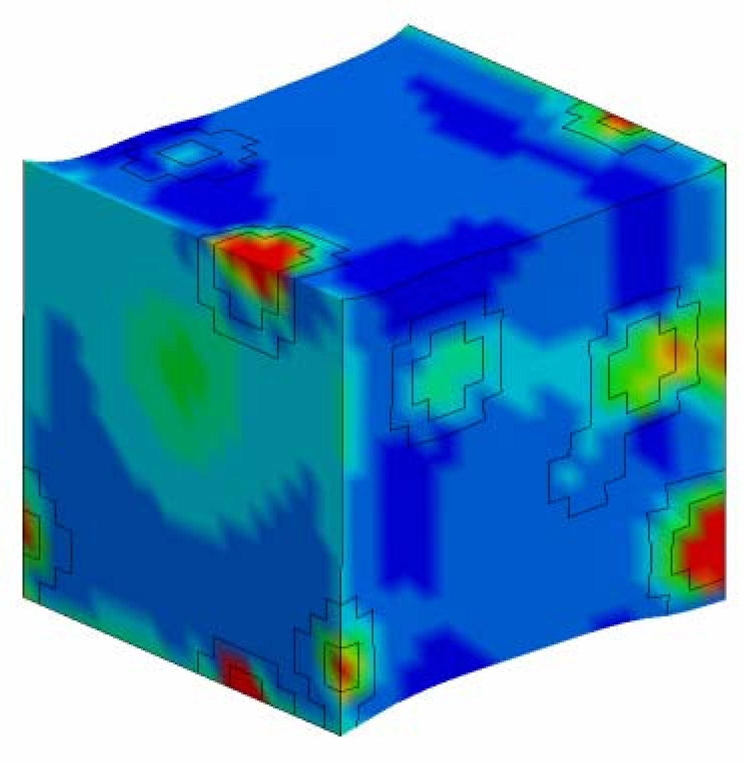

EFG implicit

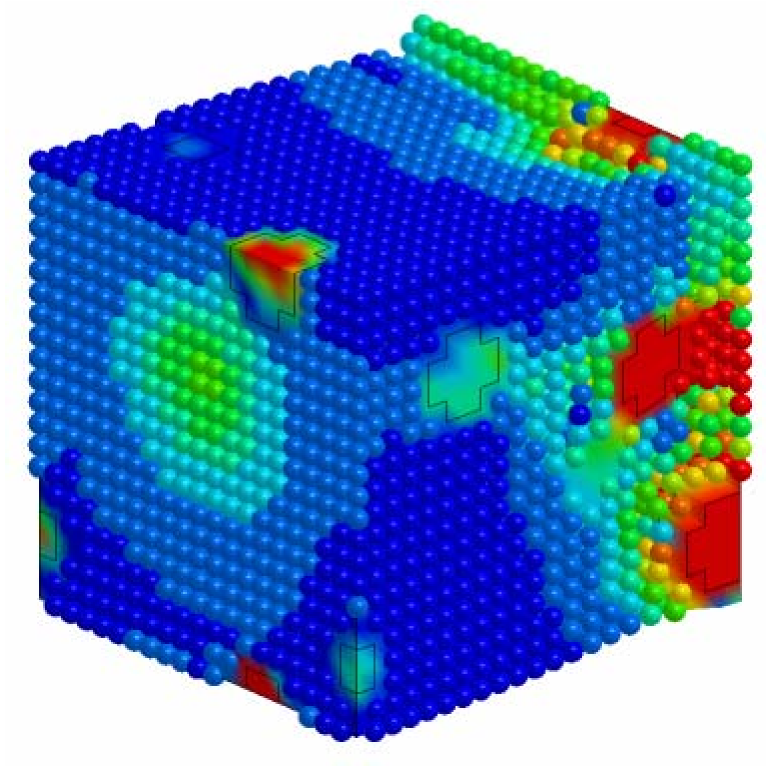

SPG explicit

Partical reinforced rubber material

Pressure Contour

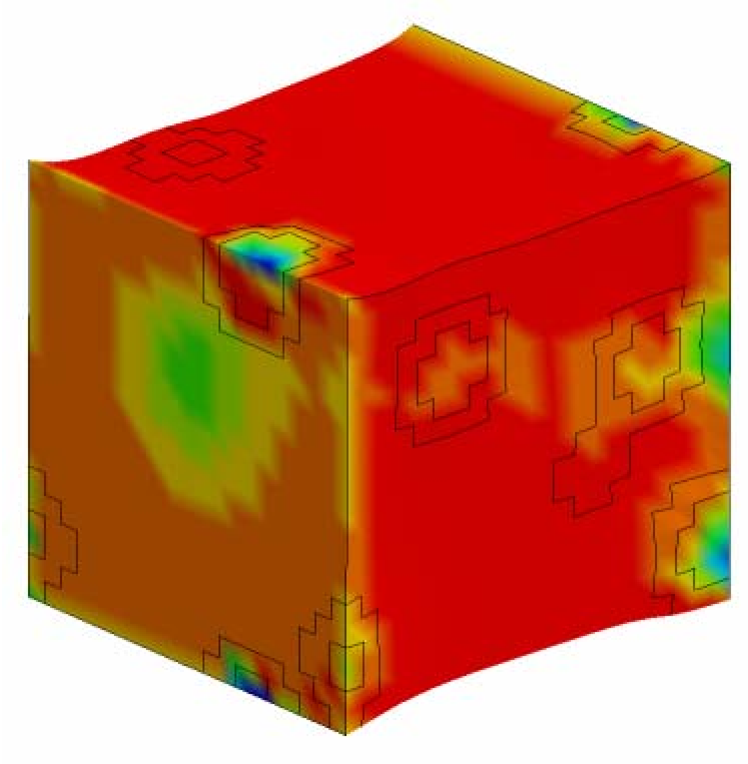

EFG implicit

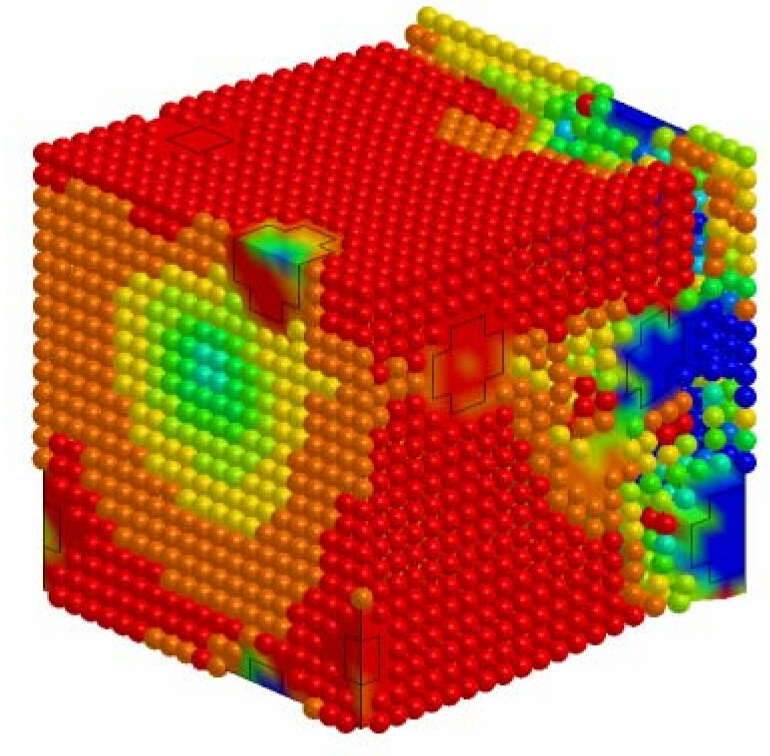

SPG explicit

Partical reinforced rubber material

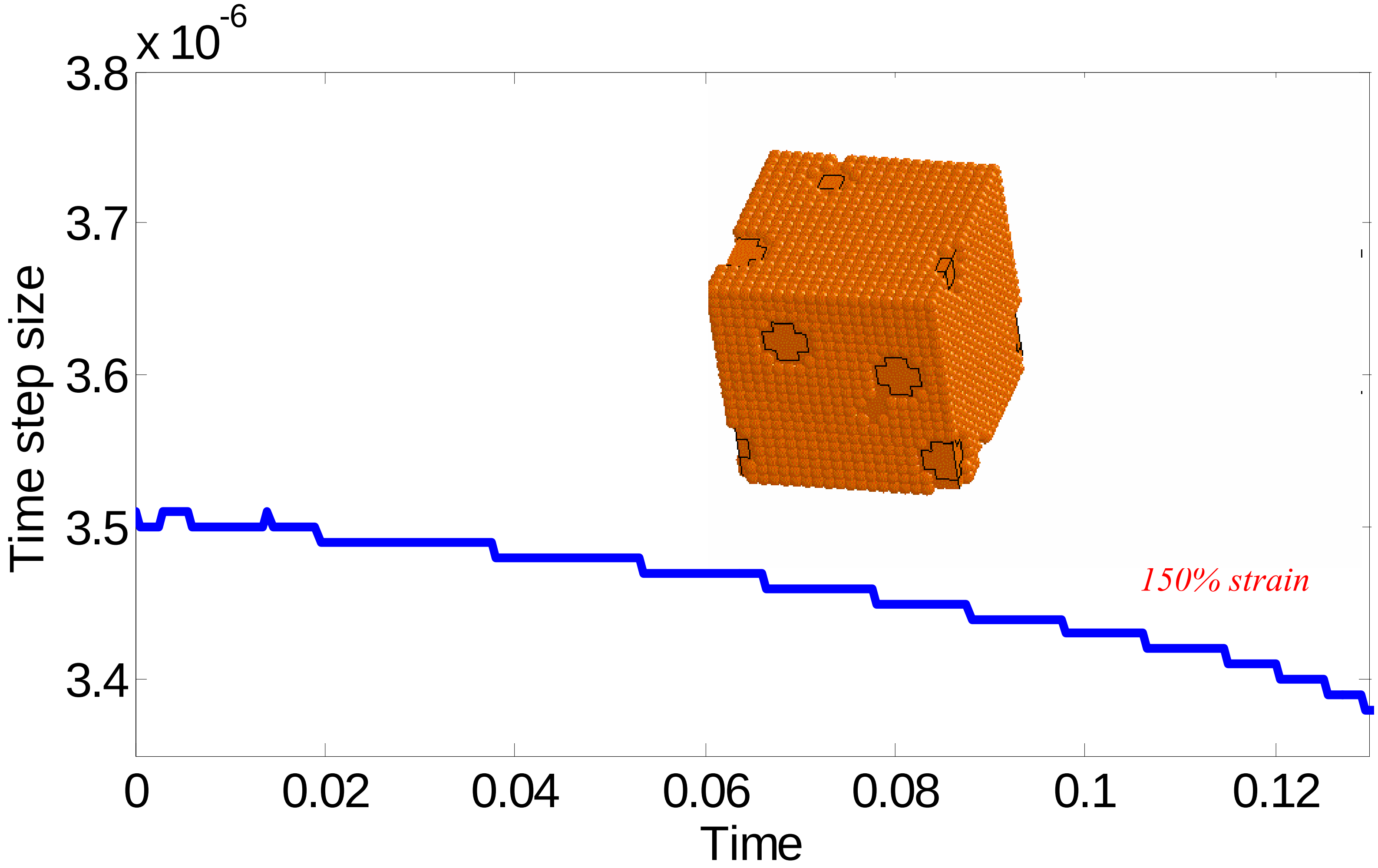

Conclusions

- Thermo-mechanical complexity and severe material flow
  - Numerical challenges:

    Large deformation, free-surface representation, high-gradient field, long CPU time, …

- Two-way Adaptive Meshfree Galerkin Method
  - GMF convex meshfree approximation
    - High order accuracy, Weak Kronecker-delta property, Minimize mesh sensitivity
  - Bypass numerical difficulty caused by abortion of adaptive mesh generation
  - Meet the requirement suggested by Neto ***[2013]*** for FSW analysis
    - Consideration of rotational boundary condition
    - Consideration frictional contact
    - Support for very high levels of deformation
    - Support for elastic-plastic or elastic-viscoplastic material models
    - Support for complex geometry

Conclusions (Cont.)

- Smoothed Particle Galerkin (SPG) Method is developed to handle severe deformation involving material failure for various solid applications.
- Official SMP and MPP versions are ready to be released in this year.
- The extension to adaptive FEM/EFG method will be considered.
- The switch from FEM to SPG method for severe deformation analysis will be implemented.

Thank you!